A)

B)

C)


Figure 2. Structures of the caged compounds Bhc-2 (10) and Bmc-2 (11) and their photochemical properties. A) Representation of photochemical cleavage of the caged compounds 2. B) UV spectra of 2 (gray line), Bhc-2 (thick black line), and Bmc-2 (thin black line). C) Plots of one-photon photolysis experiments. The plots show Bhc-2 remaining (▲), Bhc-2 product (▼), Bmc-2 remaining (●), and Bmc-2 product (■).)

scope. Of the synthetic compounds in this study, Bhc-2 was most suitable for the purpose in terms of the efficiency of the photolysis reaction and rapid translocation of PKCδ. Translocation and reactivation of kinase activity by uncaged Bhc-2 were confirmed (Figure S4).

To elucidate PKC-related signal transduction by stimulation of ligand binding, spatially and temporally controlled activation is desirable. To assess this point, photoirradiation at a limited region of interest (ROI) in the cell was performed. Because photolysis will only unblock caged ligand located in the irradiated region, the response following the activation should reflect this time- and location-dependent generation of active ligand. As shown in Figure 3, translocation was observed at

A)   B)   C)   D)

E)
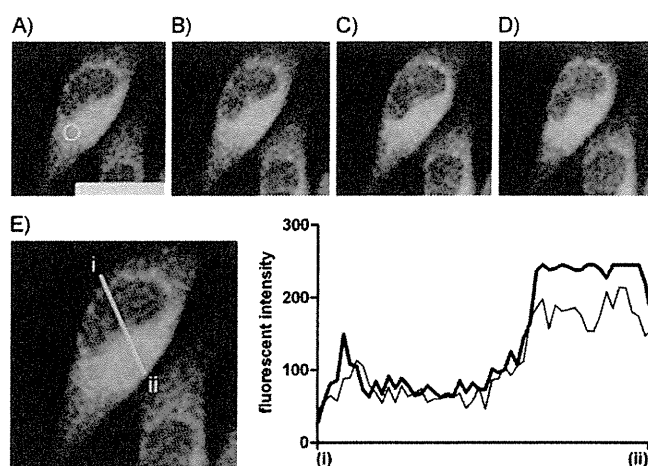
Figure 3. Translocation activated by photolysis of Bhc-2 (10). The region of interest (ROI) is limited to the inside of the circle [orange in (A)]. The panels show the translocation of EGFP-PKCδ fusion protein in a time-course as follows: A) before photoirradiation, B) 2 min, C) 5 min, and D) 10 min after photoirradiation. The image in each panel shows EGFP fluorescence. The scale bar indicates 20 μm. The detailed pictures with pseudocolors are given in Figure S5. E) Fluorescent intensity mapped along the orange bar from (i) to (ii) in the panel. The thin and thick lines show the intensity at 0 and 10 min of photoirradiation, respectively.

PKC, the carbonyl oxygen of the DAG-lactone interacts with Gly253 of PKCδ, and the hydrogen and oxygen of the hydroxy group interact with Leu251 and Thr242, respectively. In the sn-2 binding mode, which is known to be preferred by DAG-lactones, the acyl group is proposed to interact with the lipid bilayer of the cellular membranes. In this mode, the caged hydroxy group cannot interact with Leu 251 or Thr242. The caged DAG-lactones thus successfully displayed "loss of function" in binding, a requisite property of caged compounds. To examine the effects on translocation of PKCδ in mammalian cells, the caged compounds Bhc-2 and Bmc-2 were added to medium at 10 μM, a concentration at which compound 2 caused rapid translocation. Consistently with their loss of binding affinity for PKCδ, as shown by the in vitro analysis, the caged compounds failed to induce PKCδ translocation, confirming that the activation of PKCδ by compound 2 is successfully retarded by caging (Figure S3). The behavior of Bhc-2 (10) upon photolysis was also evaluated under the confocal micro-

10 min after photoirradiation of Bhc-2 (10). The pattern of subcellular localization was similar to that of compound 2 as shown in Figure 1. However, the time-course of translocation was dramatically slower, taking 10 min, in contrast with the rapid response seen upon addition of compound 2. We conclude that the photolysis of compound Bhc-2 was successful, in that translocation was observed. The slow kinetics are consistent with the concentration of the released DAG-lactone 2 being relatively low, which would be expected because the photolysis reaction occurred in the limited area of the ROI. Additionally, the cells around the ROI target cell also showed translocation of PKCδ. This effect might be caused by the release of uncaged compound and its reuptake by surrounding cells. The DAG-lactones are highly lipophilic, with their computed logP values ranging from 3 to 5. This property allows DAG-lactones to complete the hydrophobic surface of the C1b domain of PKCδ and to interact with the lipid bilayer of the membrane. However, the lipophilicity of the DAG-lactones also

— 259 —

allows the compounds to permeate through membranes and to be released back into the medium, making them available for reuptake.

It has been shown that patterns and kinetics of translocation of activated PKCδ depend on the lipophilicity and side-chain structures of DAG-lactones.[8] For compound 2, it was possible that the translocation caused is to the Golgi apparatus, because the activated PKCδ is accumulated to the perinuclear region. To confirm the translocation to the Golgi apparatus, cellular staining by BODIPY TR ceramide was performed on CHO-K1 cells expressing PKCδ-EGFP. Compound 2 was added to these cells at 10 μM. After 10 min of compound addition, the amount of PKCδ that had colocalized with Golgi apparatus was increased (Figure S6). In the next study to determine the differences in translocation between cell lines, A549 and HeLa were utilized in addition to CHO-K1 cells. As shown in Figure 4, photoirradiation induced translocation of PKCδ in all cell lines. In comparison with the stimulation by compound 2, translocation was modest because of the low concentration of released compound 2 as discussed above. Of the cell types examined, HeLa cells showed most distinctive translocation to Golgi apparatus and nuclear membrane.

In this study, the Bhc- and Bmc-caged DAG-lactones were prepared and evaluated in terms of photochemical control of PKC activation. DAG-lactone binding to PKCδ in mammalian cells was successfully controlled through photoirradiation. Derivatization at the DAG-lactone hydroxy group was shown to be very effective for diminishing affinity towards PKC. Photoactivation limited to the ROI was successfully regulated. However, there remained effects on other cells near the cells of interest, and this needs to be addressed in future studies. Development of more precise photochemical control methodology will be needed to address the signaling mechanism related to PKCδ in a single cell or at a single location within a single cell. Nonetheless, these results indicate the potential of this approach for studying PKC function.[1b,c]

Acknowledgements

Figure 4. Observation of translocation of activated PKCδ within the Golgi-stained cells by photolysis of Bhc-2 (10) in ROI. The cells are: A) CHO-K1, C) A549, and E) HeLa. The ROI is limited to the inside of the orange circles. Each set of cell images shows before photoirradiation (top) and 10 min after (bottom); EGFP-PKCδ, staining by BODIPY TR ceramide, merged image, and differential interference contrast (DIC) from left to right. The scale bars indicate 20 μm. B), D), and F) Fluorescent intensities mapped along the orange bars from (i) to (ii) in the panels. The thin and thick lines show the intensity at 0 and 10 min of photoirradiation, respectively.

— 260 —
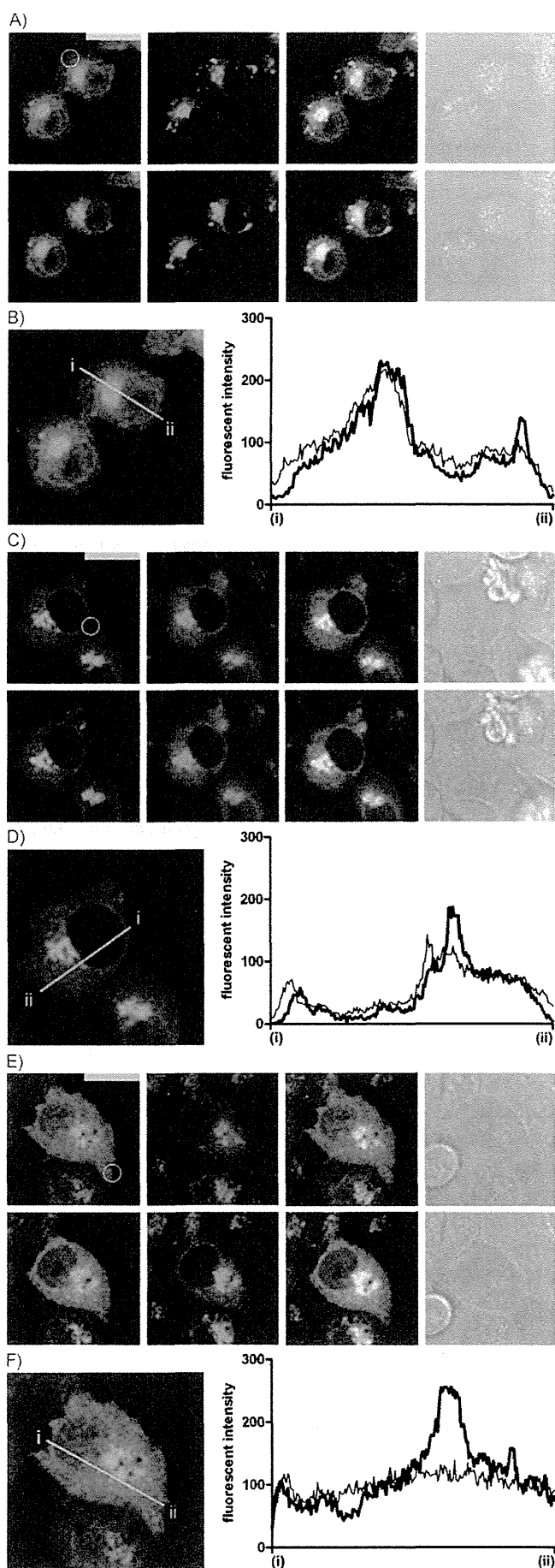
Keywords: cage compounds · diacylglycerol · drug design · enzymes · proteins

[1] a) G. Dormán, G. D. Prestwich, *Trends Biotechnol.* **2000**, *18*, 64–77; b) G. Mayer, A. Heckel, *Angew. Chem.* **2006**, *118*, 5020–5042; *Angew. Chem. Int. Ed.* **2006**, *45*, 4900–4921; c) H.-M. Lee, D. R. Larson, D. S. Lawrence, *ACS Chem. Biol.* **2009**, *4*, 409–427; d) E. J. Quann, E. Merino, T. Furuta, M. Huse, *Nat. Immunol.* **2009**, *10*, 627–637.

[2] a) Y. Nishizuka, *Science* **1992**, *258*, 607–614; b) A. C. Newton, *J. Biol. Chem.* **1995**, *270*, 28495–28498.

[3] T. Watanabe, Y. Ono, Y. Taniyama, K. Hazama, K. Igarashi, K. Ogita, U. Kikkawa, Y. Nishizuka, *Proc. Natl. Acad. Sci. USA* **1992**, *89*, 10159–10163.

[4] H. Mischak, J. H. Pierce, J. Goodnight, M. G. Kazanietz, P. M. Blumberg, J. F. Mushinski, *J. Biol. Chem.* **1993**, *268*, 20110–20115.

[5] C. Li, E. Wernig, M. Leitges, Y. Hu, Q. Xu, *FASEB J.* **2003**, *17*, 2106–2108.

[6] a) T. Ghayur, M. Hugunin, R. V. Talanian, S. Ratnofsky, C. Quinlan, Y. Emoto, P. Pandey, R. Datta, Y. Huang, S. Kharbanda, H. Allen, R. Kamen, W. Wong, D. Kufe, *J. Exp. Med.* **1996**, *184*, 2399–2404; b) D. L. Alkon, M.-K. Sun, T. J. Nelson, *Trends Pharmacol. Sci.* **2007**, *28*, 51–60.

[7] Q. J. Wang, *Trends Pharmacol. Sci.* **2006**, *27*, 317–323.

[8] V. E. Marquez, P. M. Blumberg, *Acc. Chem. Res.* **2003**, *36*, 434–443.

[9] a) K. Nacro, B. Bienfait, J. Lee, K.-C. Han, J.-H. Kang, S. Benzaria, N. E. Lewin, D. K. Bhattacharyya, P. M. Blumberg, V. E. Marquez, *J. Med. Chem.* **2000**, *43*, 921–944; b) H. Tamamura, B. Beinfait, K. Nacro, N. E. Lewin, P. M. Blumberg, V. E. Marquez, *J. Med. Chem.* **2000**, *43*, 3210–3217.

[10] a) T. Furuta, S. S.-H. Wang, J. L. Dantzker, T. M. Dore, W. J. Bybee, E. M. Callaway, W. Denk, R. Y. Tsien, *Proc. Natl. Acad. Sci. USA* **1999**, *96*, 1193–1200; b) H. Ando, T. Furuta, R. Y. Tsien, H. Okamoto, *Nat. Genet.* **2001**, *28*, 317–325; c) H. J. Montgomery, B. Perdicakis, D. Fishlock, G. A. Lajoie, E. Jervis, J. G. Guillemette, *Bioorg. Med. Chem.* **2002**, *10*, 1919–1927; d) W. Lin, D. S. Lawrence, *J. Org. Chem.* **2002**, *67*, 2723–2726; e) M. Lu, O. D. Fedoryak, B. R. Moister, T. M. Dore, *Org. Lett.* **2003**, *5*, 2119–2122; f) A. Z. Suzuki, T. Watanabe, M. Kawamoto, K. Nishiyama, H. Yamashita, M. Ishii, M. Iwamura, T. Furuta, *Org. Lett.* **2003**, *5*, 4867–4870.

[11] T. Furuta, T. Watanabe, S. Tanabe, J. Sakyo, C. Matsuba, *Org. Lett.* **2007**, *9*, 4717–4720.

[12] a) X. P. Huang, R. Sreekumar, J. R. Patel, J. W. Walker, *Biophys. J.* **1996**, *70*, 2448–2457; b) V. G. Robu, E. S. Pfeiffer, S. L. Robia, R. C. Balijepalli, Y. Pi, T. J. Kamp, J. W. Walker, *J. Biol. Chem.* **2003**, *278*, 48154–48161.

[13] a) Y. Kishi, R. R. Rando, *Acc. Chem. Res.* **1998**, *31*, 163–172; b) P. A. Wender, C. M. Cribbs, K. F. Koehler, N. A. Sharkey, C. L. Herald, Y. Kamano, G. R. Petit, P. M. Blumberg, *Proc. Natl. Acad. Sci. USA* **1998**, *95*, 7197–7201; c) S. Wang, G. W. A. Milne, M. C. Nicklaus, V. E. Marquez, J. Lee, P. M. Blumberg, *J. Med. Chem.* **1994**, *37*, 1326–1338.

[14] a) H. Tamamura, D. M. Sugano, N. E. Lewin, P. M. Blumberg, V. E. Marquez, *J. Med. Chem.* **2004**, *47*, 644–655; b) K. Malolanarasimhan, N. Kedei, D. M. Sigano, J. A. Kelley, C. C. Lai, N. E. Lewin, R. J. Surawski, V. A. Pavlyukovets, S. H. Garfield, S. Wincovitch, P. M. Blumberg, V. E. Marquez, *J. Med. Chem.* **2007**, *50*, 962–978.

[15] D. M. Sigano, M. L. Peach, K. Nacro, Y. Choi, N. E. Lewin, M. C. Nicklaus, P. M. Blumberg, V. E. Marquez, *J. Med. Chem.* **2003**, *46*, 1571–1579.

[16] a) N. A. Sharkey, P. M. Blumberg, *Cancer Res.* **1985**, *45*, 19–24; b) M. G. Kazanietz, K. W. Krausz, P. M. Blumberg, *J. Biol. Chem.* **1992**, *267*, 20878–20886.

[17] L. Li, P. S. Lorenzo, K. Bogi, P. M. Blumberg, S. H. Yupsa, *Mol. Cell. Biol.* **1999**, *19*, 8547–8558.

[18] a) T. Furuta, H. Torigai, M. Sugimoto, M. Iwamura, *J. Org. Chem.* **1995**, *60*, 3953–3956; b) B. Schade, V. Hagen, R. Schmidt, R. Herbrich, E. Krause, T. Eckardt, J. Bendig, *J. Org. Chem.* **1999**, *64*, 9109–9117.

[19] a) T. Furuta, A. Momotake, M. Sugimoto, M. Hatayama, M. Iwamura, *Biochem. Biophys. Res. Commun.* **1996**, *228*, 193–198; b) T. Furuta, M. Iwamura, *Methods Enzymol.* **1998**, *291*, 50–63.

[20] T. Eckardt, V. Hagen, B. Schade, R. Schmidt, C. Schweitzer, J. Bendig, *J. Org. Chem.* **2002**, *67*, 703–710.

[21] a) V. Hagen, J. Bendig, S. Frings, T. Eckardt, S. Helm, D. Reuter, U. B. Kaupp, *Angew. Chem.* **2001**, *113*, 1077–1080; *Angew. Chem. Int. Ed.* **2001**, *40*, 1045–1048; b) V. Hagen, S. Frings, J. Bendig, D. Lorenz, B. Wiesner, U. B. Kaupp, *Angew. Chem.* **2002**, *114*, 3775–3777; *Angew. Chem. Int. Ed.* **2002**, *41*, 3625–3628.

[22] a) D. Geißler, W. Kresse, B. Wiesner, J. Bendig, H. Kettenmann, V. Hagen, *ChemBioChem* **2003**, *4*, 162–170; b) V. Hagen, S. Frings, B. Wiesner, S. Helm, U. B. Kaupp, J. Bendig, *ChemBioChem* **2003**, *4*, 434–442.

Fluorescent-Responsive Synthetic C1b Domains of Protein Kinase Cδ as Reporters of Specific High-Affinity Ligand Binding

Nami Ohashi,[†] Wataru Nomura,*,[†] Tetsuo Narumi,[†] Nancy E. Lewin,[‡] Kyoko Itotani,[†] Peter M. Blumberg,[‡] and Hirokazu Tamamura*,[†]

Department of Medicinal Chemistry, Institute of Biomaterials and Bioengineering, Tokyo Medical and Dental University, 2-3-10 Kandasurugadai, Chiyoda-ku, Tokyo 101-0062, Japan, and Laboratory of Cancer Biology and Genetics, Center for Cancer Research, National Cancer Institute, National Institutes of Health, Bethesda, Maryland 20892, United States. Received September 18, 2010; Revised Manuscript Received December 3, 2010

Protein kinase C (PKC) is a critical cell signaling pathway involved in many disorders such as cancer and Alzheimer-type dementia. To date, evaluation of PKC ligand binding affinity has been performed by competitive studies against radiolabeled probes that are problematic for high-throughput screening. In the present study, we have developed a fluorescent-based binding assay system for identifying ligands that target the PKC ligand binding domain (C1 domain). An environmentally sensitive fluorescent dye (solvatochromic fluorophore), which has been used in multiple applications to assess protein-binding interactions, was inserted in proximity to the binding pocket of a novel PKCδ C1b domain. These resultant fluorescent-labeled δC1b domain analogues underwent a significant change in fluorescent intensity upon ligand binding, and we further demonstrate that the fluorescent δC1b domain analogues can be used to evaluate ligand binding affinity.

INTRODUCTION

Protein kinase C (PKC) is a family of serine/threonine protein kinases comprising 11 isozymes divided into three subclasses, termed conventional (α, $\beta_{I/II}$, γ), novel (δ, ε, η, θ), and atypical (ζ, λ, ι). Their classification is based on their essential structures and affinities for regulatory factors such as diacylglycerol (DAG) and calcium that bind to the C1 and C2 domains, respectively, of PKC. PKC plays a pivotal role in physiological responses to growth factors, oxidative stress, and tumor promoters (phorbol esters). These responses regulate numerous cellular processes (*1*, *2*), including proliferation (*3*), differentiation (*4*), migration (*5*), and apoptosis (*6*, *7*). The extensive involvement of PKC in both normal physiology and in numerous disorders has caused PKC to emerge as an important therapeutic target (*8–10*). Since PKC activation is regulated through the binding of ligands to its C1 domains, development of useful ligands targeted to the C1 domains has been of intense interest for medicinal chemists. Various synthetic PKC ligands based on γ-lactone templates have been developed and evaluated (*11–13*). On the other hand, since structures of many of the potent, naturally occurring PKC ligands such as the phorbol esters are highly complex, it has been difficult to extensively probe their structure–activity relationships. Much opportunity therefore remains for the development of ligands optimized for isozyme selectivity or other properties. Fluorescent-based methods possess many advantages for high-throughput screening. Especially, utilization of environmentally sensitive fluorophores is suitable for high-throughput techniques because washing steps are not generally required. Fluorophores often respond to the environmental changes in hydrophobic/hydrophilic states associated with the conformational changes of proteins accompanying ligand binding. Several screening methods based on fluorescent-modified peptides, e.g., an IP$_3$ sensor, have been developed to date (*14–17*). In this study, fluorescent-labeled C1b domains of PKCδ utilizing a solvatochromic dye as a sensor of ligand binding were designed and synthesized as efficient screening tools to evaluate ligand binding and to explore novel PKC pharmacophores.

EXPERIMENTAL PROCEDURES

General Methods. For chromatography, Wakogel C-200 (Wako Pure Chemical Industries, Ltd.) was employed. ^{1}H NMR and ^{13}C NMR spectra were recorded using a Bruker Ultrashield Plus Avance 400 spectrometer. Relative chemical shifts were reported in δ (ppm) in DMSO-d_6 or in CDCl$_3$ with tetramethylsilane as an internal standard. Low- and high-resolution mass spectra were recorded on a JMS-T1000LC AccuTOF and Bruker Daltonics microTOF-2focus. RP-HPLC was performed with linear gradients of acetonitrile and H$_2$O containing 0.1% (v/v) TFA (column: Cosmosil $_5$C$_{18}$ AR-II (4.6 × 250 mm) for analytical runs, Cosmosil $_5$C$_{18}$ AR-II (20 × 250 mm) for preparative runs. UV absorbance spectra were recorded on a Jasco V-650 spectrophotometer using a 1.0 cm path length quartz cuvette. Fluorescent spectra were recorded on a Jasco FP-6600 spectrofluorometer using a 1.0 cm path length quartz cuvette. Measurements of fluorescent intensity on 96-well plates were performed on a Wallac ARVO MX (Perkin-Elmer).

Peptide Synthesis. The protected peptide of δC1b(247–281) was manually constructed on a Novasyn TGR resin (0.25 mmol/g) by standard Fmoc-based solid phase peptide synthesis (SPPS). Fmoc-protected amino acid derivatives (5 equiv) were successively condensed using 1,3-diisopropylcarbodiimide (DIPCI) (5 equiv) in the presence of 1-hydroxybenzotriazole·H$_2$O (HOBt·H$_2$O) (5 equiv) in DMF (2 mL) (90 min treatment). The following side-chain protecting groups were used: Boc for Lys; Pbf for Arg; OBu^t for Asp; Trt for Asn, Cys, and His; Bu^t for Ser, Thr, and Tyr. The Fmoc group was deprotected with 20% (v/v) piperidine in DMF (2 mL) for 15 min. The resulting protected peptide was cleaved from the resin and deprotected with TFA-thioanisole-*m*-cresol-triisopropylsilane (TIS) (89:7.5: 2.5:1, v/v) (90 min treatment). Deprotected peptides were

* To whom correspondence should be addressed. E-mail: nomura.mr@tmd.ac.jp; tamamura.mr@tmd.ac.jp. Phone: +81-3-5280-8036. Fax: +81-3-5280-8039.
  [†] Tokyo Medical and Dental University.
  [‡] National Institutes of Health.

washed with cold Et_2O three times. The product was then purified by RP-HPLC. The protected peptides of dansyl-labeled $\delta C1b(221-246)$ were manually elongated on an Fmoc-His(Trt)-Trt(2-Cl)-resin (0.42 mmol/g) by Fmoc-based SPPS as in the synthesis of $\delta C1b(247-281)$. The following side-chain protecting groups were used: Boc for Lys; Pbf for Arg; OBu^t for Asp, Glu; Trt for Asn, Cys, Gln, and His; Bu^t for Ser, Thr, and Tyr. At the dansyl-labeled position, Fmoc-Lys(DnsGly)-OH was used. The resulting protected peptides were cleaved from the resin with trifluoroethanol (TFE)-AcOH-DCM (1:1:3, v/v) (2 h treatment), followed by thioesterification. Deprotection was performed as in the synthesis of $\delta C1b(247-281)$. The product was then purified by RP-HPLC. Mass data and chemical yields of these peptides are described in Supporting Information.

Thioesterification. Thioesterification was performed with ethyl mercaptopropionate (20 equiv), HOBt·H_2O (10 equiv), and 1-(3-dimethylaminopropyl)-3-ethylcarbodiimide (EDCI)·HCl (10 equiv) in DMF (1 mL) (-20 °C, overnight). DMF was removed by evaporation, and the crude products were washed with H_2O.

Native Chemical Ligation. Dansyl-labeled $\delta C1b(221-246)$ (1.8 mg, 0.5 μmol) and the $\delta C1b(247-281)$ (1.9 mg, 0.5 μmol) were dissolved in 500 μL of 100 mM phosphate buffer (pH 8.5) containing 6 M guanidine hydrochloride (Gn·HCl) containing 2 mM EDTA and tris(2-carboxyethyl)phosphine hydrochloride (TCEP·HCl) (1.4 mg, 5 μmol). Thiophenol (15 mL, 3%) was then added to the mixture. The ligation reaction was performed at 37 °C under an N_2 atmosphere. Progress of the ligation reaction was monitored by RP-HPLC (gradient: 25−45% of acetonitrile/0.1% TFA against $H_2O/0.1$% TFA). The product was subjected to gel filtration with Sephadex G-10 and then purified by RP-HPLC. Mass data of these peptides are described in Supporting Information.

Folding of $\delta C1b$ Domains. Purified peptides were dissolved in 50 mM Tris·HCl (pH 7.4) with 5 mM DTT, incubated for 15 min at 30 °C, and then stored at -20 °C with 20% glycerol. The peptide solution was dialyzed against 50 mM Tris·HCl (pH 7.4) containing 150 mM NaCl, 1 mM DTT, and 0.1 mM $ZnCl_2$ using a Slide-A-Lyzer Dialysis Cassette 2000 MWCO (Thermo Scientific).

[^{3}H]PDBu Binding Assay. [^{3}H]PDBu binding to the $\delta C1b$ domains was measured using the poly(ethylene glycol) precipitation assay as described previously (*18, 19*) with minor modifications. To determine the dissociation constants (K_d) and numbers of binding sites (B_{max}) for the dansyl-labeled $\delta C1b$ domains, saturation curves with increasing concentrations of [^{3}H]PDBu were obtained in triplicate. 250 μL of the assay mixture contained 50 mM Tris·HCl (pH 7.4), 1 mM ethylenebis(oxyethylenenitrilo)tetraacetic acid (EGTA), 0.1 mg/mL phosphatidylserine, 5 mg/mL bovine immunoglobulin G, variable concentrations of [^{3}H]PDBu, and, for those tubes used to determine nonspecific binding, an excess of nonradioactive PDBu. After addition of peptides stored in 0.015% Triton X-100, binding was carried out at 18 °C for 10 min. Samples were incubated on ice for 10 min. 200 μL of 35% poly(ethylene glycol) in 50 mM Tris·HCl (pH 7.4) was added, and the samples were incubated on ice for an additional 10 min. The tubes were centrifuged at 4 °C (12 200 rpm, 15 min), and a 100 μL aliquot of each supernatant was then transferred to a scintillation vial for determination of the amount of the free [^{3}H]PDBu. After the remaining supernatant was aspirated off, the bottom of each centrifuge tube was cut off just above the pellet and transferred to a scintillation vial for the determination of the amount of the total bound [^{3}H]PDBu. Dissociation constants (K_d) were calculated by Scatchard analysis.

CD Measurement. CD spectra were recorded on a Jasco J-720 spectropolarimeter at 25 °C. The measurements were

performed at 0.1 nm spectral resolution using a 0.5 cm path length quartz cuvette. Each spectrum represents the average of 40 scans, and the scan rate was 100 nm/min. Measurements were performed in a Tris·HCl (pH 7.4) buffer containing 1 mM DTT and 150 mM NaCl.

Fluorescence Measurement. Ligand titration was performed in 1 mL of dialysis buffer containing 0.5 μM dialyzed dansyl-labeled $\delta C1b$ domain and 5 μg/mL phosphatidylserine at 25 °C. After each addition of ligands, the mixture was incubated at the same temperature for 10 min. Fluorescent emission spectra ($\lambda_{ex} = 330$ nm; slit width: 20 nm for excitation, 40 nm for emission) were obtained throughout the addition of ligands. For experiments using 96-cell plates, Dansyl-labeled $\delta C1b$ domain solution (dialysis buffer containing 0.5 μM dialyzed peptides and 5 μg/mL phosphatidylserine) was prepared and incubated for 10 min at room temperature. Fluorescence of dansyl-labeled $\delta C1b$ domain was measured using an excitation filter of 355 nm (half-width: 40 nm) and an emission filter of 460 nm (half-width: 25 nm), respectively.

Molecular Modeling. Molecular modeling was performed using Sybyl 7.1 (Tripos Inc., St. Louis, MO). Predictive models of dansyl-labeled $\delta C1b$ domain analogues were built by substitution of Lys(Dns-Gly) for residues Tyr238, Ser240, or Thr242 that were contained in the crystal structure of $\delta C1b$ domain (PDB 1PTR) (*20*). Energy-minimization was performed on the Lys(Dns-Gly) moiety using the Tripos force field and Gasteiger-Huckel charge parameters.

RESULTS AND DISCUSSION

Design of Fluorescent-Labeled PKCδ C1b Domains. Residues 221−281 of PKCδ forming the C1b domain represent the starting sequence we used for modification. To identify the optimal amino acid position for fluorescent labeling, Tyr238, Ser240, and Thr242 were selected for evaluation. Our choice was based on the following rationale: First, these residues are located at the edge of the binding pocket of the C1b domain as shown by the structure of $\delta C1b$-phorbol ester complex (*20*). Second, site-directed mutagenesis had shown that Ser240 was not necessary for the phorbol ester binding and that the $\delta C1b$ domain mutants T242G, T242S, and T242 V had only minimal effects on the binding affinity of PDBu (2.1-, 1.1-, and 3.2-fold, respectively) (*21*). Third, replacement of Tyr by Gly in position 238 reduced binding affinity of [^{3}H]PDBu by 60-fold, but maintained nanomolar affinity ($K_d = 48 \pm 3.0$ nM), which might be sufficient for the detection of PKC ligands (*21*). A chemically modified lysine was utilized for fluorescent labeling. For this study, a dansyl group was adopted because of its small molecular size and larger Stokes shift compared to NBD (*22*). Since the flexibility of the dansyl moiety might contribute to its sensitivity to ligand binding to the $\delta C1b$ domain, glycine was incorporated between the ε-amino group of lysine and the dansyl moiety as a linker to construct Lys(Dns-Gly) (Supporting Information Scheme S1). Three $\delta C1b$ domain analogues, in which Lys(Dns-Gly) was substituted for Tyr238, Ser240, or Thr242, were designed and designated as Y238K(DnsG), S240K(DnsG), and T242K(DnsG), respectively. Predictive structural models of the dansyl-labeled $\delta C1b$ domains were constructed based on the crystal structure of the $\delta C1b$ domain (PDB entry 1PTR) utilizing Sybyl 7.1 (Figure 1). The models showed that the dansyl moieties of S240K(DnsG) and T242K(DnsG) are located outside the binding pocket, whereas the dansyl moiety of Y238K(DnsG) was located inside.

Synthesis of Dansyl-Labeled $\delta C1b$ Domain Analogues. Fmoc-protected Lys(Dns-Gly) (**4**) was synthesized as described in Supporting Information Scheme S1. $\delta C1b$ domain analogues were synthesized based on the standard Fmoc solid-phase peptide synthesis (SPPS) (*23*). For an efficient synthesis of
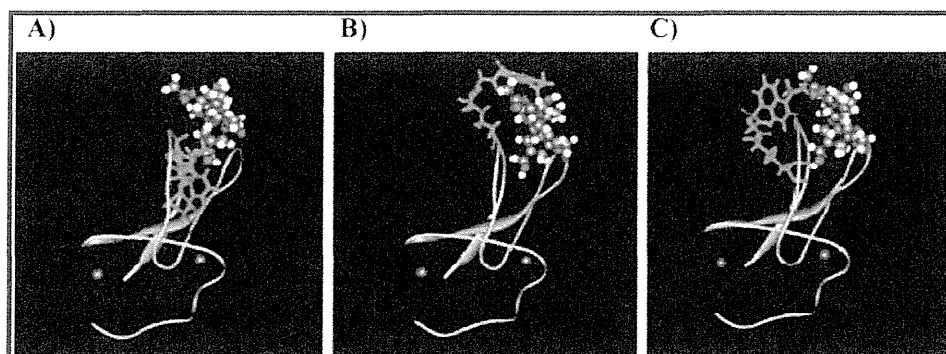
Figure 1. Structural models of dansyl-labeled δC1b analogues. (A) Y238K(DnsG), (B) S240K(DnsG), and (C) T242K(DnsG). Space-filling models indicate phorbol esters and zinc atoms.
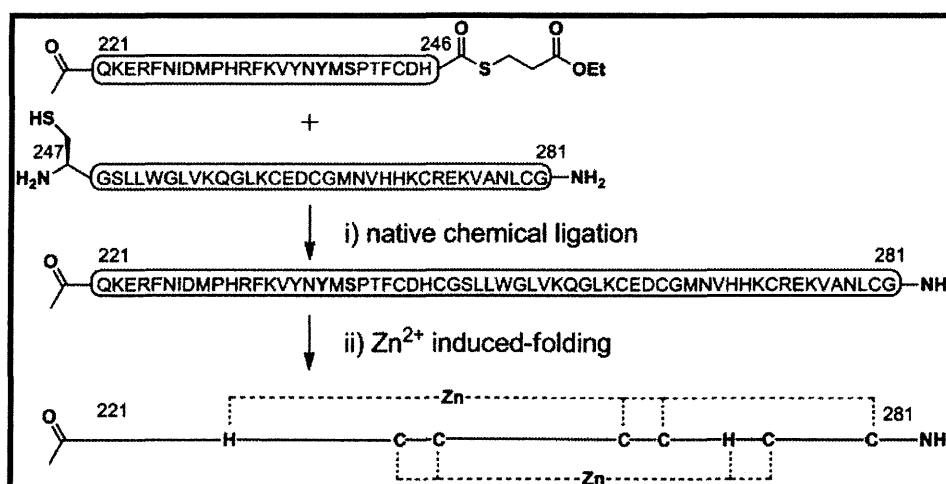
Figure 2. Schematic representation of construction of dansyl-labaled δC1b. (i) 100 mM phosphate buffer (pH 8.5), 6 M Gn·HCl, 2 mM EDTA, TCEP·HCl, thiophenol, N_2, 37 °C; (ii) 50 mM Tris·HCl (pH 7.4), 150 mM NaCl, 1 mM DTT, 0.1 mM $ZnCl_2$, 4 °C.

dansyl-labeled δC1b domain analogues, a native chemical ligation (NCL) method was adopted (*18, 24*). Three N-terminal peptide fragments (dansyl-labeled δC1b(221−246)) and a common C-terminal peptide fragment (δC1b(247−281)) were separately synthesized. A purified δC1b(247−281) and three dansyl-labeled δC1b(221−246) fragments were condensed by an NCL method (Figure 2). The ligation reaction was performed with 0.8 mM of each peptide fragment in 100 mM phosphate buffer (pH 8.5) containing 6 M Gn·HCl, 2 mM EDTA, and 3% thiophenol at 37 °C. The progress of the ligation reaction was monitored by HPLC (Supporting Information). The condensed δC1b domains were identified by ESI-TOF-mass spectra (Supporting Information Table S1). The purified peptides were lyophilized and obtained as powders. Total yields of NCL were 38% for Y238K(DnsG), 48% for S240K(DnsG), and 41% for T242K(DnsG). Folding of the synthetic δC1b domain was performed by dialysis against Zn^{2+} containing buffer (50 mM Tris·HCl (pH 7.4), 150 mM NaCl, 1 mM DTT, 0.1 mM $ZnCl_2$) at 4 °C.

Characterization of Synthetic δC1b Analogues. The apparent [³H]PDBu binding affinity of the dansyl-labeled δC1b domains was evaluated by the method described previously (*18, 19*). S240K(DnsG) and T242K(DnsG) showed K_d values comparable to that of the wild type. However, B_{max} values were 6% for S240K(DnsG) and 11% for T242K(DnsG) compared to the wild type (Table 1). The results indicate that dansyl-labeling might partly impair the efficiency of correct folding of the synthetic δC1b domain. Y238K(DnsG) did not possess significant binding affinity for PDBu, consistent with the predictions from the modeling. We conclude that the dansyl-labeled δC1b domains maintain potent binding activity and correct folding, at least for an appreciable proportion of the

Table 1. Binding Activity of the Synthetic δC1b Analogues to [³H]PDBu

| peptides	K_d (nM)^a	B_{max} (pmol/mg)^b
wild type	0.34 ± 0.08	38000
Y238K(DnsG)	n.d.^{c}	11
S240K(DnsG)	0.18 ± 0.05	2100
T242K(DnsG)	0.35 ± 0.04	3700

^{a} Dissociation constant for the synthetic δC1b binding to [³H]PDBu. Mean ± SEM. ^{b} Numbers of binding sites. ^{c} Not determined.

product, in those cases in which the dansyl group is located outside the binding pocket.

To estimate the influence of dansyl-labeling on folding of δC1b domain, circular dichroism (CD) spectroscopy of S240K(DnsG) and T242K(DnsG) was performed for comparison before and after dialysis (Figure 3). Since the CD spectrum of the synthetic δC1b(231−281) is similar to that of the recombinant δC1b domain (*18*), Y238K(DnsG)-δC1b(231−281) was used to evaluate the effects of dansyl-labeling on folding of Y238K(DnsG) (Supporting Information Figure S3). The addition of $ZnCl_2$ did not cause a significant change of CD spectra of Y238K(DnsG)-δC1b(231−281). Thus, the introduction of a dansyl group into Tyr238 might interfere correct folding. The CD spectra of both of the dansyl-labeled δC1b domains before dialysis showed broad minima around 205 nm, suggesting random coil structures (*25*). CD spectra of the dialyzed dansyl-labeled δC1b domains exhibited decreases of negative cotton effects around 205 nm, which were similar to those of recombinant and synthetic δC1b domains (*18, 25*).

The apparent [³H]PDBu binding affinities and CD spectra of the dansyl-labeled δC1b domains, S240K(DnsG) and
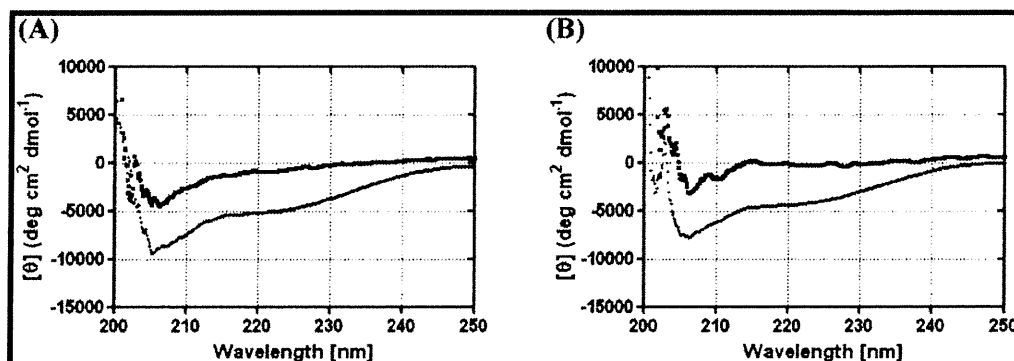
Figure 3. Changes of CD spectra of dansyl-labeled δC1b analogues, S240K(DnsG) (A) and T242K(DnsG) (B). Blue and black plots show profiles before and after dialysis against Zn^{2+} containing buffer, respectively.
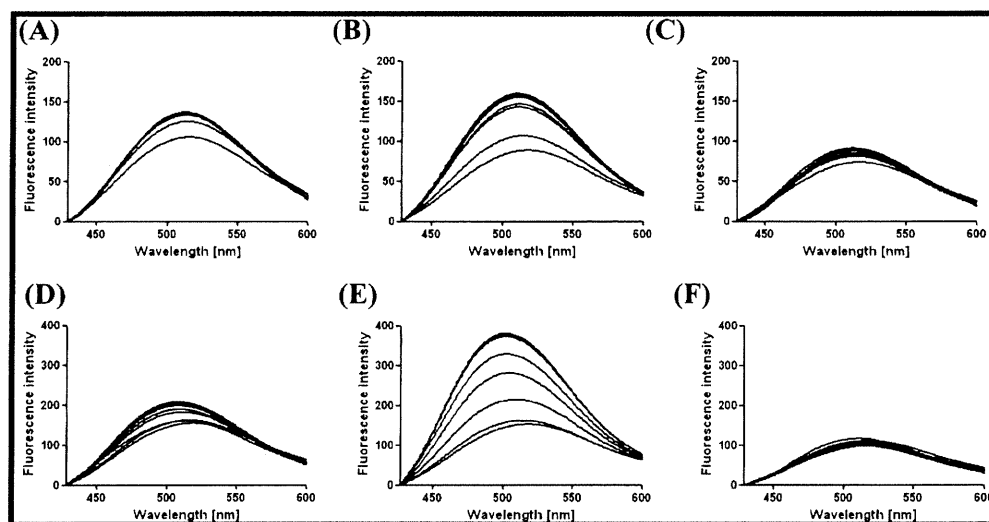

Figure 4. Fluorescent spectra obtained by ligand titration experiments for dansyl-labeled δC1b analogues. Panels A—C show titrations of PDBu, PMA, and PDA against S240K(DnsG), respectively. Panels D—F show titrations of PDBu, PMA, and PDA against T242K(DnsG), respectively. Dansyl-labeled δC1b analogue, 0.5 μM; buffer, 50 mM Tris·HCl (pH 7.4), 150 mM NaCl, 1 mM DTT, 0.1 mM $ZnCl_2$, 5 μg/mL phosphatidylserine; ligand, 0.02, 0.06, 0.1, 0.14, 0.18, 0.22, 0.26, 0.3 equiv, λ_{ex} = 330 nm.

T242K(DnsG), demonstrated that insertion of dansyl groups at Ser 240 and at Thr 242 maintained correct folding and strong ligand binding affinity comparable to that of the wild type, although involving reduction of the stability of the domains.

Titration of Ligands to Fluorescent-Labeled δC1b Domain Analogues. To evaluate the fluorescent properties of dansyl-labeled δC1b domain, fluorescent emission spectra were measured during ligand titration. As test ligands, the phorbol esters PDBu (K_i = 0.72 ± 0.06 nM), phorbol 12-myristate 13-acetate (PMA) (K_i = 0.14 ± 0.04 nM), and phorbol 12,13-diacetate (PDA) (K_i = 68.9 ± 5.9 nM), were employed. Values of K_i were determined by competitive binding assays using [³H]PDBu (Supporting Information). Fluorescent titration experiments showed that the spectra of the dansyl-labeled δC1b domain analogues changed according to the ligand concentration. S240K(DnsG) showed 1.3-, 1.8-, and 1.2-fold increases in fluorescent intensity and blue shifts in the emission maxima upon additions of PDBu, PMA, and PDA, respectively (Figures 4A—C). T242K(DnsG) showed 1.3-, 2.6-, and 1.1-fold increases in fluorescent intensity and blue shifts in the emission maxima upon additions of PDBu, PMA, and PDA, respectively (Figures 4D—F). The rank order of increases in fluorescent intensity upon addition of the above ligands to S240K(DnsG) and T242K(DnsG) thus corresponded to that of their K_i values.

Since dansyl-Gly showed stronger fluorescent intensity in a hydrophobic environment than in a hydrophilic environment

(Supporting Information Figure S1), the increases in fluorescence intensity upon ligand titration of S240K(DnsG) and T242K(DnsG) suggested that the environment surrounding the dansyl moiety was changed to become more hydrophobic upon ligand binding (26–28). As predicted in the modeling study, the dansyl group was not located in the binding pocket, preventing binding. Even after ligand binding, the dansyl group will still be located outside the binding pocket. Thus, the binding of ligands to the binding pocket must make the environment surrounding the dansyl more hydrophobic, possibly due to interactions between dansyl and the long alkyl chains of the ligands. In addition, T242K(DnsG) showed stronger fluorescence intensity than did S240K(DnsG). This phenomenon corresponds to their relative B_{max} values observed in the [³H]PDBu binding assay (Figures 1B, C, Table 1). A reason could be the hydrogen bonding network at the binding site of phorbol ester on the δC1b domain. The C20 hydroxy group of the phorbol ester accepts a hydrogen bond from the main-chain NH of T242 (20). Thus, the stronger fluorescent intensity of T242K(DnsG) could be due to a closer distance to the bound ligand. Furthermore, saturation of the increase in fluorescent intensity was observed when the ligand concentration reached 0.05–0.1 μM (10–20% of the peptide concentration) (Figure 5). This result is consistent with the B_{max} values of dansyl-labeled δC1b: 6–11% of the wild type. The K_d values based on titration of ligands to the dansyl-labeled δC1b domains were evaluated (Table 2). As a control experiment, S240K(DnsG) dialyzed without Zn^{2+} did not
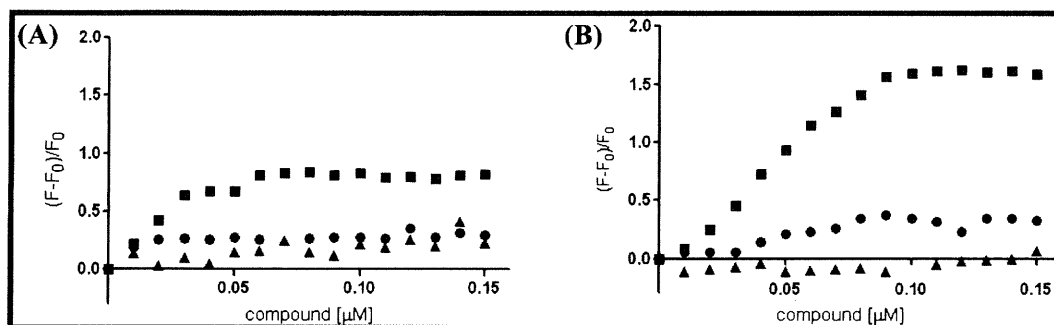
Figure 5. Plots of change of fluorescence intensity from titration experiments using S240K(DnsG) (A) and T242K(DnsG) (B). Dansyl-labeled δC1b analogue, 0.5 μM; square, PMA; round, PDBu; triangle, PDA.
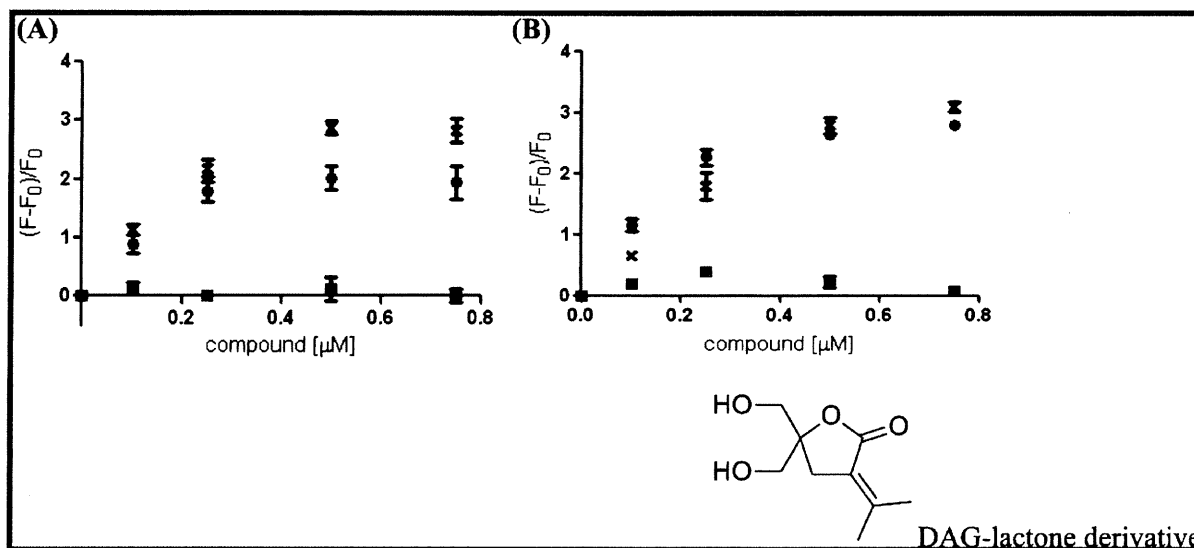
Figure 6. Plots of change of fluorescence intensity from 96-well plates-based titration experiments of S240K(DnsG) (A) and T242K(DnsG) (B). cross, PMA; circle, PDBu; square, DAG-lactone derivative.

Table 2. K_d **Values of the Fluorescent-Labeled** δC1b **Domain Analogues Based on Titration of Ligands**

compound	S240K(DnsG) K_d (nM)[a]	T242K(DnsG) K_d (nM)[a]
PMA	20.6	121.6
PDBu	5.83	110
PDA	Not convergent	Not fitting

[a] Dissociation constant for the fluorescent-labeled δC1b domain analogues to each compound was calculated.

show any significant increase in fluorescent intensity upon the addition of PDBu (Supporting Information Figure S2), suggesting that correct folding involving zinc-finger formation is critical for ligand binding. The detection limit might be the level of the fluorescent intensity of PDA. The results of titration experiments indicate that, upon ligand binding to correctly folded C1b domains, the site surrounding the ligand binding pocket becomes more hydrophobic. Even if some uncertainty remains about the relative contributions of the mechanisms leading to this change in hydrophobicity, the core finding is that ligand binding was detected by an increase in fluorescent intensity, which corresponds to binding affinity. The binding activity of ligands can be possibly evaluated by increases in fluorescent intensity upon the consideration of LogP values.

S240K(DnsG) and T242K(DnsG) were employed in fluorescent experiments utilizing 96-well plates for initial assessment of their suitability to high-throughput screening. Plots of changes of fluorescent intensity against the ligand concentration showed dose-dependent curves similar to those in titration experiments (Figure 6). The results indicate that the present fluorescent-

responsive C1b domains can be used for screening of novel PKC pharmacophores.

CONCLUSIONS

In this study, three kinds of dansyl-labeled δC1b domains, Y238K(DnsG), S240K(DnsG), and T242K(DnsG), were synthetically constructed in an efficient way by utilizing Fmoc-SPPS and an NCL method. The results of CD measurements and [³H]PDBu binding assays indicated that the position of dansyl-labeling was critical for maintenance of native functions including proper folding. The ligand titration of dansyl-labeled δC1b showed that the change of fluorescent spectra corresponded to the K_i values of the ligands. Furthermore, S240K(DnsG) and T242K(DnsG) were utilized for measurements using a 96-well plate-based format, indicating that evaluation of ligand binding could be performed in a high-throughput fashion. The present fluorescent-responsive domains were successfully utilized in vitro. However, through optimization of the stability of the fluorescent-labeled δC1b domain, these domains might also be adapted for cell-based assays as efficient DAG sensors.

Supporting Information Available: Detailed materials and methods. This material is available free of charge via the Internet at http://pubs.acs.org.

LITERATURE CITED

(1) Nishizuka, Y. (1992) Intracellular signaling by hydrolysis of phospholipids and activation of protein kinase C. *Science 258*, 607–614.

(2) Newton, A. C. (1995) Protein kinase C: structure, function, and regulation. *J. Biol. Chem. 270*, 28495–28498.

(3) Watanabe, T., Ono, Y., Taniyama, Y., Hazama, K., Igarashi, K., Ogita, K., Kikkawa, U., and Nishizuka, Y. (1992) Cell division arrest induced by phorbol ester in CHO cells overexpressing protein kinase C-delta subspecies. *Proc. Natl. Acad. Sci. U.S.A. 89*, 10159–10163.

(4) Mischak, H., Pierce, J. H., Goodnight, J., Kazanietz, M. G., Blumberg, P. M., and Mushinski, J. F. (1993) Phorbol ester-induced myeloid differentiation is mediated by protein kinase C-alpha and -delta and not by protein kinase C-beta II, -epsilon, -zeta, and -eta. *J. Biol. Chem. 268*, 20110–20115.

(5) Li, C., Wernig, E., Leitges, M., Hu, Y., and Xu, Q. (2003) Mechanical stress-activated PKCdelta regulates smooth muscle cell migration. *FASEB J. 17*, 2106–2108.

(6) Ghayur, T., Hugunin, M., Talanian, R. V., Ratnofsky, S., Quinlan, C., Emoto, Y., Pandey, P., Datta, R., Huang, Y., Kharbanda, S., Allen, H., Kamen, R., Wong, W., and Kufe, D. (1996) Proteolytic activation of protein kinase C delta by an ICE/CED 3-like protease induces characteristics of apoptosis. *J. Exp. Med. 184*, 2399–2404.

(7) Humphries, M. J., Limesand, K. H., Schneider, J. C., Nakayama, K. I., Anderson, S. M., and Reyland, M. E. (2006) Suppression of apoptosis in the protein kinase Cdelta null mouse in vivo. *J. Biol. Chem. 281*, 9728–9737.

(8) Alkon, D. L., Sun, M. K., and Nelson, T. J. (2007) PKC signaling deficits: a mechanistic hypothesis for the origins of Alzheimer's disease. *Trends Pharmacol. Sci. 28*, 51–60.

(9) Churchill, E., Budas, G., Vallentin, A., Koyanagi, T., and Mochly-Rosen, D. (2008) PKC isozymes in chronic cardiac disease: possible therapeutic targets? *Annu. Rev. Pharmacol. Toxicol. 48*, 569–599.

(10) O'Brian, C. A., Ward, N. E., Stewart, J. R., Chu, F., Mackay, H. J., and Twelves, C. (2001) Prospects for targeting protein kinase C isozymes in the therapy of drug-resistant cancer—an evolving story. *Cancer Metastasis Rev. 20*, 95–100.

(11) Tamamura, H., Sigano, D. M., Lewin, N. E., Blumberg, P. M., and Marquez, V. E. (2004) Conformationally constrained analogues of diacylglycerol. 20. The search for an elusive binding site on protein kinase C through relocation of the carbonyl pharmacophore along the sn-1 side chain of 1,2-diacylglycerol lactones. *J. Med. Chem. 47*, 644–655.

(12) Tamamura, H., Sigano, D. M., Lewin, N. E., Peach, M. L., Nicklaus, M. C., Blumberg, P. M., and Marquez, V. E. (2004) Conformationally constrained analogues of diacylglycerol (DAG). 23. Hydrophobic ligand-protein interactions versus ligand-lipid interactions of DAG-lactones with protein kinase C (PK-C). *J. Med. Chem. 47*, 4858–4864.

(13) Marquez, V. E., and Blumberg, P. M. (2003) Synthetic diacylglycerols (DAG) and DAG-lactones as activators of protein kinase C (PK-C). *Acc. Chem. Res. 36*, 434–443.

(14) Morii, T., Sugimoto, K., Makino, K., Otsuka, M., Imoto, K., and Mori, Y. (2002) A new fluorescent biosensor for inositol trisphosphate. *J. Am. Chem. Soc. 7*, 1138–1139.

(15) Venkatraman, P., Nguyen, T. T., Sainlos, M., Bilsel, O., Chitta, S., Imperiali, B., and Stern, L. J. (2007) Fluorogenic probes for monitoring peptide binding to class II MHC proteins in living cells. *Nat. Chem. Biol. 3*, 201–202.

(16) Joshi, B. P., and Lee, K. H. (2008) Synthesis of highly selective fluorescent peptide probes for metal ions: tuning selective metal monitoring with secondary structure. *Bioorg. Med. Chem. 16*, 8501–8509.

(17) Simard, J. R., Grütter, C., Pawar, V., Aust, B., Wolf, A., Rabiller, M., Wulfert, S., Robubi, A., Klüter, S., Ottmann, C., and Rauh, D. (2009) High-throughput screening to Identify inhibitors which stabilize inactive kinase conformations in p38α. *J. Am. Chem. Soc. 131*, 18478–18488.

(18) Ohashi, N., Nomura, W., Kato, M., Narumi, T., Lewin, N. E., Blumberg, P. M., and Tamamura, H. (2009) Synthesis of protein kinase Cδ C1b domain by native chemical ligation methodology and characterization of its folding and ligand binding. *J. Pept. Sci. 10*, 642–646.

(19) Kazanietz, M. G., Areces, L. B., Bahador, A., Mischak, H., Goodnight, J., Mushinski, J. F., and Blumberg, P. M. (1993) Characterization of ligand and substrate specificity for the calcium-dependent and calcium-independent protein kinase C isozymes. *Mol. Pharmacol. 44*, 298–307.

(20) Zhang, G., Kazanietz, M. G., Blumberg, P. M., and Hurley, J. H. (1995) Crystal structure of the cys2 activator-binding domain of protein kinase C delta in complex with phorbol ester. *Cell 81*, 917–924.

(21) Kazanietz, M. G., Wang, S., Milne, G. W., Lewin, N. E., Liu, H. L., and Blumberg, P. M. (1995) Residues in the second cysteine-rich region of protein kinase C delta relevant to phorbol ester binding as revealed by site-directed mutagenesis. *J. Biol. Chem. 270*, 21852–21859.

(22) Soini, E., and Hemmila, I. (1979) Fluoroimmunoassay: present status and key problems. *Clin. Chem. 25*, 353–361.

(23) Irie, K., Oie, K., Nakahara, A., Yanai, Y., Ohigashi, H., Wender, P. A., Fukuda, H., Konishi, H., and Kikkawa, U. (1998) Molecular basis for protein kinase C isozyme-selective binding: the synthesis, folding, and phorbol ester binding of the cysteine-rich domains of all protein kinase C isozymes. *J. Am. Chem. Soc. 120*, 9159–9167.

(24) Dawson, P. E., Churchill, M. J., Ghadiri, M. R., and Kent, S. B. H. (1997) Chemical protein synthesis by solid phase ligation of unprotected peptide segments. *J. Am. Chem. Soc. 119*, 4325–4329.

(25) Zimenkov, Y., Dublin, S. N., Ni, R., Tu, R. S., Breedveld, V., Apkarian, R. P., and Conticell, V. P. (2006) Rational design of a reversible pH-responsive switch for peptide self-assembly. *J. Am. Chem. Soc. 128*, 6770–6771.

(26) Ikeda, H., Nakamura, M., Ise, N., Oguma, N., Nakamura, A., Ikeda, T., Toda, F., and Ueno, A. (1996) Fluorescent cyclodextrins for molecule sensing: fluorescent properties, NMR characterization, and inclusion phenomena of n-dansylleucine-modified cyclodextrins. *J. Am. Chem. Soc. 118*, 10980–10988.

(27) Ikunaga, T., Ikeda, H., and Ueno, A. (1999) The effects of avidin on inclusion phenomena and fluorescent properties of biotin-appended dansyl-modified β-cyclodextrin. *Chem.—Eur. J. 5*, 2698–2704.

(28) Matsumura, S., Sakamoto, S., Ueno, A., and Mihara, H. (2000) Construction of α-helix peptides with β-cyclodextrin and dansyl units and their conformational and molecular sensing properties. *Chem.—Eur. J. 6*, 1781–1788.

Intense Blue Fluorescence in a Leucine Zipper Assembly

Hiroshi Tsutsumi,[a, c] Seiichiro Abe,[a, b] Tomoaki Mino,[a, b] Wataru Nomura,[a] and Hirokazu Tamamura*[a, b]

Fluorescent probes are valuable molecular tools in chemical biology, and various fluorescent probes for the detection of small biological components have been developed and used for fluorescence imaging in cells.[1] Ratiometric fluorescent probes and fluorogenic probes are particularly useful because they can suppress noise associated with background emission.[2] Tag/probe pairs for the fluorescence imaging of proteins have recently been developed,[3] but the number of fluorogenically active tag/probe pairs is still limited.

Green fluorescent protein (GFP) is a widely used biological tool for the imaging of proteins in live cells.[4] Its fluorescence is well controlled because the fluorophore unit is located in a unique microenvironment inside a β-barrel structure. We have previously developed a new tag/probe pair with fluorogenic activity—based on the unique characteristics of GFP—by use of the leucine zipper assembly, the ZIP tag/probe.[5] The environment surrounding the 4-nitrobenzo-2-oxa-1,3-diazole (NBD) component of the probe peptide changes drastically from a hydrophilic state to a hydrophobic state through the formation of a 3α-helical leucine zipper structure between the tag and the probe peptides, as a result of which the bright green fluorescence of the NBD dye is induced. Use of other solvatochromic fluorophores should enable us to develop fluorogenic ZIP tag/probe pairs with other fluorescence colors. Here we describe the use of 7-diethylaminocoumarin-3-carboxylic acid (DEAC) in the development of another ZIP tag/probe pair with switchable blue fluorescence.

ZIP tag/probe pairs containing the DEAC dye were designed as described in our previous report (Scheme 1).[5] In a probe α-helical peptide, a DEAC moiety was attached to the side chain of L-α-2,3-diaminopropionic acid [Dap(DEAC)]. A Dap(DEAC) residue is situated at the X-position in the probe peptide to locate the DEAC dye in the hydrophobic region of the 3α-helical leucine zipper structure. In tag antiparallel 2α-helical peptides, two Leu residues at the Z-positions in the L2 peptide are residues complementary to the Dap(DEAC) residue of the

probe peptide, and these residues are replaced by alanine (A2 peptide) or glycine (G2 peptide) so that hydrophobic spaces can be formed when the tag peptides bind to the probe peptide.

The fluorescence spectra of the DEAC probe peptide showed a remarkable change as the concentration of the A2 peptide was increased. The emission maximum due to the DEAC dye shifted from 482 to 470 nm as the emission intensity increased (Figure 1 B). A DEAC-β-alanine methyl ester (7) showed emission maxima at 483 nm in HEPES buffer solution and at 470 nm in MeOH (see the Supporting Information). These results clearly suggest that through the formation of the DEAC probe/A2 peptide complex, the DEAC moiety of the probe peptide is moved from a hydrophilic environment in bulk water to a hydrophobic environment inside the 3α-helical bundle structure. The fluorescence intensity of the DEAC probe peptide at 470 nm increased up to 10.5 times on addition of A2 in a typical saturation manner (Figure 2 A, Table 1).

Table 1. Emission maxima, $\Delta I_{max}/I_0$ values (in parentheses), and relative fluorescent quantum yields of the probe peptide and tag/probe complexes, the dissociation constants (K_d) between the tag and the probe peptides, and the α-helical contents of the probe, the tag peptides, and their complexes (in parentheses).

	Probe	L2	A2	G2
λ_{max} ($\Delta I_{max}/I_0$)	482 nm (–)	466 nm (3.4)	470 nm (10.5)	457 nm (51.7)
$\phi_r^{[a]}$	1	5.56	17.7	39.2
$K_d^{[b]}$	–	94.0 nM[d]	2.29 nM[e]	250 nM[f]
α-helix content[c]	60%	81% (78%)	58% (76%)	19% (72%)

[a] Relative fluorescent quantum yield at 430 nm excitation. [b] Measurement conditions: HEPES buffer solution [pH 7.2, 50 mM, NaCl (100 mM)], 25 °C, [probe] = 0.5 μM. [c] Measurement conditions: Tris-HCl buffer solution [pH 7.2, 50 mM, NaCl (100 mM)], 25 °C, [tag], [probe], [tag/probe] = 1.0 μM. The α-helical contents were determined by a standard method. [d]–[f] Determined from the fluorescent intensity changes at 466, 470, or 457 nm, respectively.
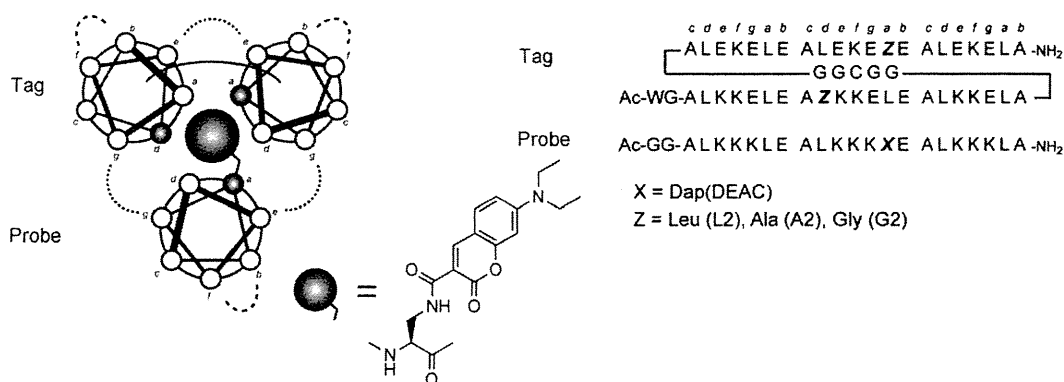
[a] Dr. H. Tsutsumi, S. Abe, T. Mino, Dr. W. Nomura, Prof. H. Tamamura
Institute of Biomaterials and Bioengineering
Tokyo Medical and Dental University
Chiyoda-ku, Tokyo 101-0062 (Japan)

[b] S. Abe, T. Mino, Prof. H. Tamamura
School of Biomedical Science, Tokyo Medical and Dental University
Chiyoda-ku, Tokyo 101-0062 (Japan)
Fax: (+81)3-5280-8039
E-mail: tamamura.mr@tmd.ac.jp

[c] Dr. H. Tsutsumi
Present address: Department of Synthetic Chemistry and
Biological Chemistry, Graduate School of Engineering
Kyoto University Katsura
Kyoto, 615-8510 (Japan)

The fluorescent intensity of the DEAC probe/A2 peptide complex at 470 nm is about eight times higher than that of compound 7 in MeOH and the complex showed a similar fluorescent spectrum to that of compound 7 in acetone. These results indicate that the microenvironment in the DEAC probe/A2 peptide complex might be more hydrophobic than MeOH. The shift of the emission maximum of the L2 peptide, from 482 to 466 nm, was slightly larger than that of the DEAC probe/A2 peptide pair, but the fluorescence intensity change was lower than that in the case of the A2 peptide (3.4 times at 466 nm; Figure 1 A, Table 1). This result implies that the small fluorescent change in the DEAC probe/L2 peptide complex might be

```
                          c d e f g a b   c d e f g a b   c d e f g a b
                   Tag   ┌ALEKELE ALEKEZE ALEKELA-NH₂
                         │          GGCGG
                         Ac-WG-ALKKELE AZKKELE ALKKELA┘

                   Probe   Ac-GG-ALKKKLE ALKKKXE ALKKKLA-NH₂

                         X = Dap(DEAC)
                         Z = Leu (L2), Ala (A2), Gly (G2)
```

Scheme 1. Structures and amino acid sequences of ZIP tag/probe pairs containing DEAC dye.
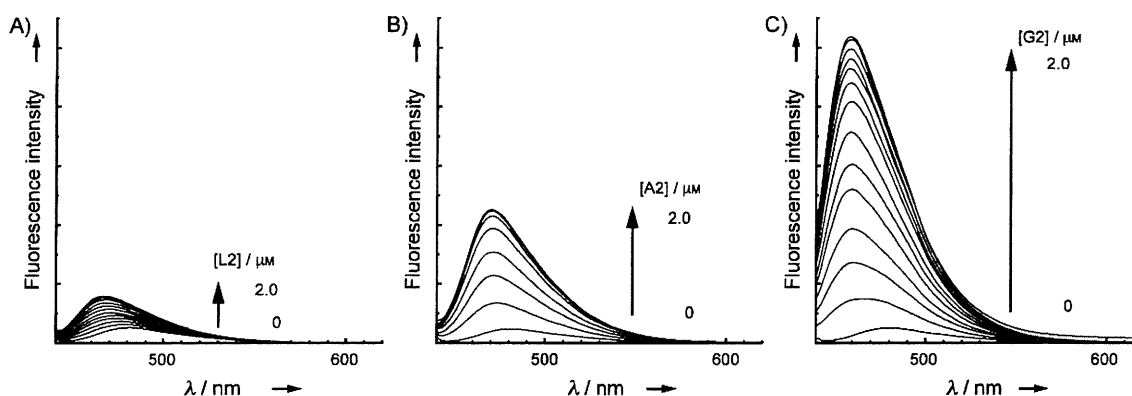

Figure 1. Fluorescence spectral change of the DEAC probe peptide upon addition of A) L2, B) A2, and C) G2 at 25 °C in HEPES buffer [pH 7.2, 50 mM, NaCl (100 mM)]: [probe]=0.5 μM, λ_{ex}=430 nm.

caused by a lack of space to accommodate the DEAC dye. Interestingly, the addition of the G2 peptide to the DEAC probe peptide induced a significant blue shift, from 482 nm to

Figure 2. A) Fluorescence titration curves of the DEAC probe peptide with L2, A2, and G2 at 466, 470, and 457 nm, respectively. *I* represents the fluorescent intensity at various concentrations of tag peptides and I_0 the initial fluorescent intensity. B) Fluorescent photography of: i) the DEAC probe peptide, ii) the DEAC probe peptide/L2 complex, iii) the DEAC probe peptide/A2 complex, and iv) the DEAC probe peptide/G2 complex. [Probe]=0.5 μM, [tag]=2.0 μM.

457 nm in the emission maximum and a substantial enhancement of the fluorescent intensity at 457 nm (51.7 times; Figure 2 A, Table 1). The fluorescent spectrum of the DEAC probe/ G2 peptide complex is similar to that of compound 7 in dichloromethane (Figure S1 in the Supporting Information). These results indicate that the DEAC dye is located in an extremely hydrophobic environment in the DEAC probe/G2 peptide complex. The relative fluorescent quantum yields (ϕ_r) of the DEAC probe/A2 peptide pair and the DEAC probe/G2 peptide pair relative to the probe peptide alone are 17.7 and 39.2, respectively (Table 1). Although fluorescent quantum yields of DEAC dye derivatives in aqueous media are low,[6] these remarkable ϕ_r increases enable the naked eye to detect the fluorescent change (Figure 2 B).
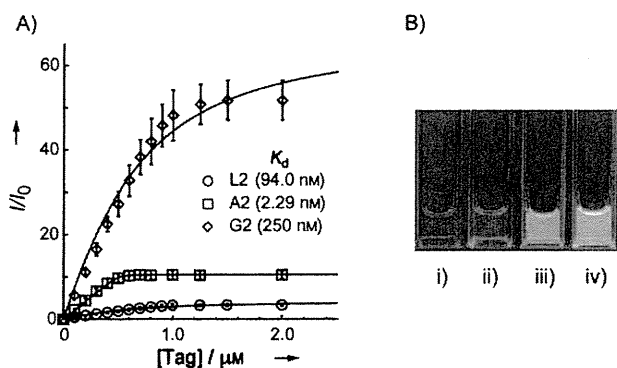
In the circular dichroism (CD) study, the L2, A2, and DEAC probe peptides showed CD spectral patterns typical of α-helical structures, with negative maxima at 208 and 222 nm, whereas the G2 peptide, in contrast, showed a random coil pattern (Figure 3). The α-helical contents of L2, A2, G2, and the DEAC probe peptides were determined to be 81, 58, 19, and 60%, respectively, by a standard method (Table 1).[7] The α-helical content of the DEAC probe peptide/A2 complex is estimated as 76%, which is higher than those of the DEAC probe pep-

— 269 —
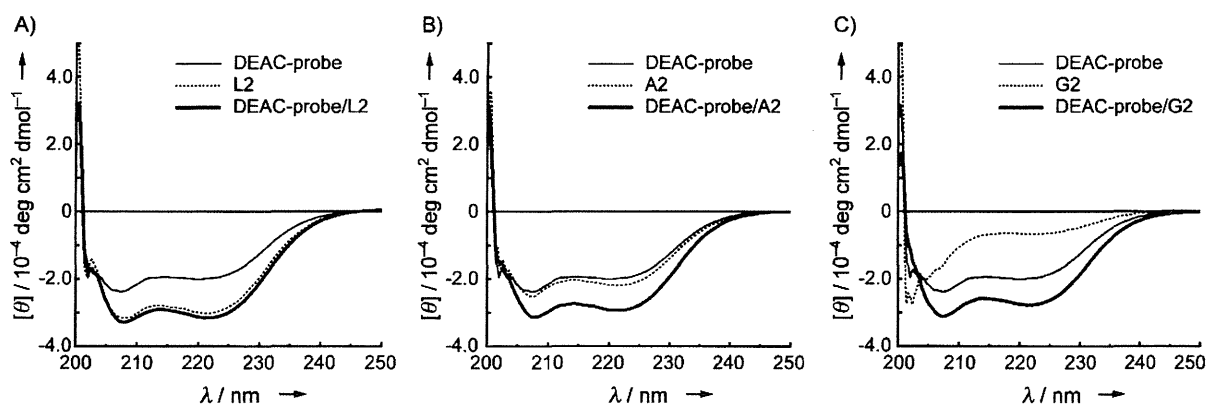
Figure 3. Circular dichroism spectra of tag and the DEAC probe peptides at 25°C in Tris-HCl buffer [pH 7.2, 50 mM, NaCl (100 mM)]. A) The DEAC probe peptide (solid line), L2 (dashed line), and the complex of probe/L2 (bold solid line). B) The DEAC probe peptide (solid line), A2 (dashed line), and the complex of probe/A2 (bold solid line). C) The DEAC probe peptide (solid line), G2 (dashed line), and the complex of probe/G2 (bold solid line).

tide or the A2 peptide alone, suggesting that more stable α-helical structures are induced in the DEAC probe/A2 peptide complex through the formation of the 3α-helical leucine zipper structure. Enhancement of the α-helical structure of the DEAC probe peptide was also observed in the DEAC probe/L2 peptide complex, with an α-helical content of 78%. Interestingly, a similar enhancement of α-helical structure was observed in the DEAC probe/G2 peptide complex (72%) but the α-helical content of the G2 peptide was only 19%. The G2 peptide has two glycine residues, which destabilize α-helix structures generally, and this is presumably the reason for its lower α-helix content. On the other hand, the G2 peptide might easily be folded into a stable α-helical structure by complexation with the DEAC probe peptide in the induced fit manner. This result clearly suggests that the DEAC probe/G2 peptide pair can also form a stable 3α-helical structure. The shape of the hydrophobic space formed in the DEAC probe/G2 peptide complex might fit well to the DEAC dye and as a result, the DEAC dye would be tightly fixed in the hydrophobic space and the bright blue fluorescence would result.

The apparent dissociation constants (K_d) of the DEAC peptide with the L2, A2, and G2 peptides were determined to be 93.9 nM, 2.29 nM, and 250 nM, respectively, by a nonlinear least-squares curve fitting method based on a 1:1 stoichiometry model[8] (Table 1), and so the binding affinities of the L2 and A2 peptides for the DEAC probe peptide were higher than that of the G2 peptide. The L2 and A2 peptides showed high α-helix contents before complexation with the DEAC probe peptide, but the G2 peptide, in contrast, showed a random coil structure. These results suggest that the prefolded α-helix structure of the L2 and A2 peptides is important for the high-affinity binding to the DEAC probe peptide. However, the binding affinity between the G2 peptide and the DEAC probe peptide is thought to be sufficiently strong as a tag/probe pair for protein labeling. In addition, a cross-linking strategy might be useful to compensate the binding affinity of the G2 peptide and the DEAC probe peptide. We have recently reported cross-link-type ZIP tag/probe pairs based on covalent bond forma-

tion that enhances the binding affinities and the complex stabilities of tag probe pairs.[5b]

In conclusion, we have developed leucine zipper tag/probe pairs with blue fluorogenic activity. The weak fluorescence seen in the DEAC probe peptide alone is greatly intensified through binding with the A2 or G2 tag peptides. In particular, the G2 peptide induces a greater than 50-fold fluorescence enhancement of the DEAC probe peptide concurrently with a large blue shift of the emission maximum. The G2 peptide binds to the DEAC probe peptide in an induced fit manner, which appears to be essential for the remarkable fluorescent change. The fluorescence enhancement of the DEAC probe peptide induced by the binding to the A2 and G2 peptides can easily be detected by the naked eye. Pairs of the DEAC probe peptide and the A2 or G2 peptides are thus new ZIP tag/probe pairs with blue turn-on fluorescence.

Keywords: coumarin · fluorescence · imaging agents · leucine zipper · peptides

[1] a) Topics in Fluorescence Spectroscopy, Vol. 9: Advanced Concepts in Fluorescence Sensing, Part A: Small Molecule Sensing (Eds.: C. D. Geddes, J. R. Lakowicz), Springer, New York, 2005; b) Topics in Fluorescence Spectroscopy, Vol. 10: Advanced Concepts in Fluorescence Sensing, Part B: Macromolecular Sensing (Eds.: C. D. Geddes, J. R. Lakowicz), Springer, New York, 2005.

[2] a) T. Terai, T. Nagano, Curr. Opin. Chem. Biol. 2008, 12, 515–521; b) G. Grynkiewwicz, M. Poenie, R. Y. Tsien, J. Biol. Chem. 1985, 260, 3440–3450; c) A. Ojida, I. Takashima, T. Kohira, H. Nonaka, I. Hamachi, J. Am. Chem. Soc. 2008, 130, 12095–12101.

[3] a) B. A. Griffin, S. R. Adams, R. Y. Tsien, Science 1998, 281, 269–272; b) E. G. Guignet, R. Hovius, H. Vogel, Nat. Biotechnol. 2004, 22, 440–444; c) A. Ojida, K. Honda, D. Shinmi, S. Kiyonaka, Y. Mori, I. Hamachi, J. Am. Chem. Soc. 2006, 128, 10452–10459; d) A. Keppler, S. Gendreizig, T. Gronemeyer, H. Pick, H. Vogel, K. Johnsson, Nat. Biotechnol. 2002, 21, 86–89; e) K. Stöhr, D. Siegberg, T. Ehrhard, K. Lymperopoulos, S. Öz, S. Schulmeister, A. C. Pfeifer, J. Bachmann, U. Klingmüller, V. Sourjik, D.-P. Herten, Anal. Chem. 2010, 82, 8186–8193; f) G. V. Los, A. Darzins, N. Karassina, C. Zimprich, R. Learish, M. G. McDougall, L. P. Encell R. Friedman-Ohana, M. Wood, G. Vidurgiris, Promega Cell Notes 2005, 11, 2–6; g) S. Mizukami, S. Watanabe, Y. Hori, K. Kikuchi, J. Am. Chem. Soc. 2009, 131, 5016–5017.

[4] a) O. Shimomura, F. H. Johnson, Y. Saiga, *J. Cell. Comp. Physiol.* **1962**, *59*, 223–229; b) M. Zimmer, *Chem. Rev.* **2002**, *102*, 759–781; c) R. Y. Tsien, *FEBS Lett.* **2005**, *579*, 927–932.

[5] a) H. Tsutsumi, W. Nomura, S. Abe, T. Mino, A. Masuda, N. Ohashi, T. Tanaka, K. Ohba, N. Yamamoto, K. Akiyoshi, H. Tamamura, *Angew. Chem.* **2009**, *121*, 9328–9330; *Angew. Chem. Int. Ed.* **2009**, *48*, 9164–9166; b) W. Nomura, T. Mino, T. Narumi, N. Ohashi, A. Masuda, C. Hashimoto, H. Tsutsumi, H. Tamamura, *Biopolymers* **2010**, *94*, 843–852.

[6] K. Azuma, S. Suzuki, S. Uchiyama, T. Kajiro, T. Santa, K. Imai, *Photochem. Photobiol. Sci.* **2003**, *2*, 443–449.

[7] D. Y. Jackson, D. S. King, J. Chmielewski, S. Singh, P. G. Schultz, *J. Am. Chem. Soc.* **1991**, *113*, 9391–9392.

[8] T. Kuwabara, A. Nakamura, A. Ueno, F. Toda, *J. Phys. Chem.* **1994**, *98*, 6297–6303.

— 271 —

CHEMMEDCHEM

DOI: 10.1002/cmdc.201000548

Azamacrocyclic Metal Complexes as CXCR4 Antagonists

Tomohiro Tanaka,[a] Tetsuo Narumi,*[a] Taro Ozaki,[a] Akira Sohma,[a] Nami Ohashi,[a] Chie Hashimoto,[a] Kyoko Itotani,[a] Wataru Nomura,[a] Tsutomu Murakami,[b] Naoki Yamamoto,[b, c] and Hirokazu Tamamura*[a]

The chemokine receptor CXCR4 is a member of the seven transmembrane GPCR family, which is implicated in multiple diseases, including HIV infection, cancers, and rheumatoid arthritis. Low-molecular-weight nonpeptidic compounds, including AMD3100 and various pyridyl macrocyclic zinc(II) complexes, have been identified as selective antagonists of CXCR4. In the present study, structure–activity relationship studies were performed by combining the common structural features of alkylamino and pyridiyl macrocyclic antagonists. Several new zinc(II) or copper(II) complexes demonstrated potent anti-HIV activity, strong CXCR4-binding activity, and significant inhibitory activity against Ca^{2+} mobilization induced by CXCL12 stimulation. These results may prove useful in the design of novel CXCR4 antagonists, and the compounds described could potentially be developed as therapeutics against CXCR4-relevant diseases or chemical probes to study the biological activity of CXCR4.
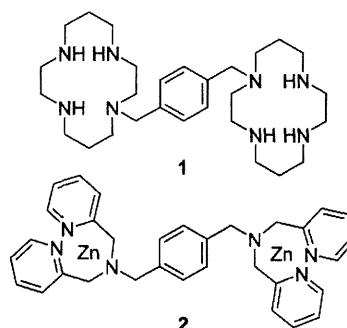
Introduction

The chemokine receptor CXCR4, which transduces signals of its endogenous ligand, CXCL12/stromal cell-derived factor-1 (SDF-1),[1–4] is classified as a member of the seven transmembrane GPCR family, and plays a physiological role via its interaction with CXCL12 in chemotaxis,[5] angiogenesis,[6,7] and neurogenesis[8,9] in embryonic stages. CXCR4 is, however, relevant to multiple diseases including HIV infection/AIDS,[10,11] metastasis of several types of cancer,[12–14] leukemia cell progression,[15,16] and rheumatoid arthritis (RA),[17,18] and is considered an attractive drug target to combat these diseases. Thus, inhibitors targeting CXCR4 are expected to be useful for drug discovery.

Several CXCR4 antagonists have been reported,[19–35] including our discovery of the highly potent CXCR4 antagonist T140, a 14-mer peptide with a disulfide bridge, its smaller derivative, the 5-mer cyclic peptide FC131, and several other potent analogues.[19,24–26,28–30] Clinical development of these peptidic antagonists could be pursued using specific administration strategies involving biodegradable microcapsules.[14,36] However, herein we focus on novel nonpeptidic low-molecular-weight CXCR4 antagonists. To date, AMD3100 (1),[20,22] Dpa-Zn complex (2),[37] KRH-1636,[27] and other compounds[31–35] have been developed in this and other laboratories as low-molecular-weight nonpeptidic CXCR4 antagonists. The present study reports structure–activity relationship studies based on the combination of common structural motifs, such as xylene scaffolds and cationic moieties that are present in the aforementioned compounds.

Results and Discussion

In order to determine spatially suitable positioning of cationic moieties, p- and m-xylenes were utilized as spacers. Cationic moieties such as bis(pyridin-2-ylmethyl)amine (dipicolylamine), 1,4,7,10-tetraazacyclododecane (cyclen), and 1,4,8,11-tetraaza-

1

2

cyclotetradecane (cyclam) were introduced as R^1 and R^2 (Figure 1). This combination of R^1, R^2, and spacer groups led to the design and synthesis of compounds 12–31.

The CXCR4 binding activity of synthetic compounds was assessed based on the inhibition of [^{125}I]CXCL12 binding to Jurkat cells, which express CXCR4.[38] The percent inhibition of all compounds at 1 μM is shown in Table 1. Seven compounds (16, 17, 20–22, 28, and 29, Table 1) resulted in greater than 87% inhibition. The high activity of 16 is consistent with re-

[a] T. Tanaka, Dr. T. Narumi, T. Ozaki, A. Sohma, N. Ohashi, C. Hashimoto, K. Itotani, Dr. W. Nomura, Prof. H. Tamamura
Institute of Biomaterials and Bioengineering
Tokyo Medical and Dental University
2-3-10 Kandasurugadai, Chiyoda-ku, Tokyo 101-0062 (Japan)
Fax: (+81)3-5280-8039
E-mail: tamamura.mr@tmd.ac.jp

[b] Dr. T. Murakami, Prof. N. Yamamoto
AIDS Research Center, National Institute of Infectious Diseases
1-23-1 Toyama, Shinjuku-ku, Tokyo 162-8640 (Japan)

[c] Prof. N. Yamamoto
Department of Microbiology, Yong Loo Lin School of Medicine
National University of Singapore, Singapore 117597 (Singapore)

Supporting information for this article is available on the WWW under http://dx.doi.org/10.1002/cmdc.201000548.

— 272 —

FULL PAPERS
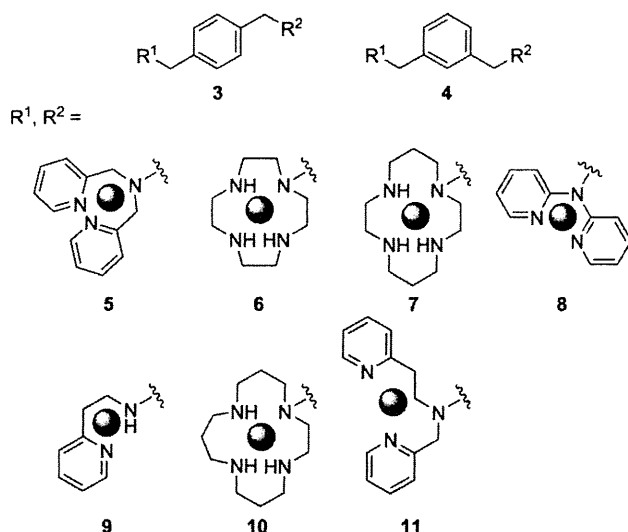
Figure 1. The structures of aromatic spacers (upper) and cationic moieties (R^1 and R^2). The shaded circle represents the position of the metal cation (Zn^{II} or Cu^{II}) in the chelate.

sults reported previously.[20,22] The anti-HIV activities of **17** and **29**, which contain only cyclam or cyclal rings, were reported by De Clercq et al.[39,40] Compounds with only pyridine and/or cyclen rings did not show any high binding activity. The presence of azamacrocyclic rings is presumably indispensable to the interaction of these compounds with CXCR4, and the size of rings appears to be important because not only compounds **16** and **17**, with two cyclam rings in the molecule, but also compounds **28** and **29**, with two cyclal rings, have remarkably more potent CXCR4 binding activity than compounds **14** and **15**, which have two cyclen rings. Compound **22**, with a p-xylene moiety, exhibited higher activity than compound **23**, which has an m-xylene moiety, indicating that p-xylene is more suitable than m-xylene as a spacer for approximate positioning of cationic moieties. At 0.1 μM, compound **22** resulted in 86% inhibition of [^{125}I]CXCL12 binding, while the other six compounds exhibited 37–66% inhibition. The IC$_{50}$ value of compound **22** was estimated to be 37 nM.

ZnCl$_2$ was added to phosphate-buffered saline (PBS) solutions of these 20 compounds, **12-31**, to form zinc(II) complexes. The percent inhibition for each compound at 1 μM against [^{125}I]CXCL12 binding was determined and is given in Table 1. Zinc complexation of **12-15, 18, 19,** and **23** resulted in a remarkable increase in CXCR4 binding activity compared to the corresponding zinc-free compounds. These molecules contain dipicolylamine and/or cyclen moieties, suggesting that chelation of the nitrogen atoms with the zinc(II) ion significantly affects their interactions with CXCR4. The high activity of the zinc chelates of **12** and **13** is consistent with results provided in our previous paper.[37] Additionally, the anti-HIV activity of zinc complexes of **14** and **15** was reported by Kimura et al.[41] For compounds with only dipicolylamine and/or cyclen macrocycles as cationic moieties (**12-15, 18,** and **19**), zinc complexation is critical to achieve high binding activity; the correspond-

ing zinc-free compounds exhibit no significant activity. Compounds **16, 17, 20-22, 28,** and **29** demonstrated high binding affinity in metal-free states as well as in zinc complexation states, indicating that zinc complexation of either of the macrocyclic rings in these compounds is not essential for high activity. The CXCR4 binding activity and anti-HIV activity of the zinc complex of **16** were reported previously.[42,43] Measured inhibition percentages for 0.1 μM of the zinc complexes of **12, 14-23, 28,** and **29** are given in Table 1. The zinc complexes of **20-22, 28,** and **29** at 0.1 μM exhibited greater than 79% inhibition of [^{125}I]CXCL12 binding, and the other eight zinc complexes (of **12, 14-19,** and **23,**) showed less than 55% inhibition. The IC$_{50}$ values of zinc complexes of **20-22, 28,** and **29** were estimated to be 11, 8.3, 22, 40, and 52 nM, respectively. Zinc complexes of compounds containing a combination of cyclen and cyclam moieties, **20** and **21**, had remarkably potent IC$_{50}$ values.

To form chelates with a copper(II) cation, CuCl$_2$ was added to solutions in PBS of **12-31**. The inhibition percentages of all the compounds at 1 μM against [^{125}I]CXCL12 binding are shown in Table 1. Copper complexes of **14** and **15** exhibited a significant increase in CXCR4 binding activity as compared to the corresponding copper-free compounds, a phenomenon which is also seen in the zinc chelates. These compounds have two cyclen moieties in the molecules, suggesting that zinc or copper complexation is critical for high binding activity. Compounds **16, 17,** and **20-22** showed high binding affinities in metal-free states and zinc- and copper-complexed states, indicating that metallic complexation of the cyclam rings in these compounds is not necessary for high activity. The CXCR4 binding activity of the copper complex of **16** was previously reported.[42] For compounds **17, 22, 23, 28,** and **29**, copper complexation caused a significant decrease in binding activity compared to the corresponding copper-free compounds, whereas for compounds **14, 15, 18,** and **19**, copper complexation caused an increase in binding activity. This phenomenon may be due to the difference in ring sizes and structures of macrocycles, and was not observed upon zinc-complex formation. Inhibition at 0.1 μM of the copper complexes of **16** and **20-22**, which exhibited greater than 85% inhibition of [^{125}I]CXCL12 binding at 1 μM, are given in Table 1. The copper complexes of **16, 20, 21,** and **22** at 0.1 μM showed 39, 69, 88, and 39% inhibition, respectively, with the IC$_{50}$ value of the copper complex of **21** estimated to be 16 nM.

Molecular modeling analysis of compound **21** and its zinc(II) and copper(II) complexes predicted that these complexes would form a stable coordinate conformation as shown in Figure 2. In general, zinc(II) complexes are predicted to adopt a tetrahedral conformation, while copper(II) complexes form a planar four coordinate/square conformation. The zinc(II) complex of **21** is predicted to have a tetrahedral conformation and the copper(II) complex a square planar conformation in both the cyclen and cyclam rings. The carboxyl group of either Asp 171 or Asp 262 in CXCR4 is thought to coordinate strongly with zinc ions but not copper ions in the complexes,[41–43] and as a consequence, the zinc complex of **21** would bind more strongly than **21** or its copper complex. This order of binding

Table 1. CXCR4 binding activity of compounds 12–31 in the metal ion-free form, the zinc complex, and the copper complex.

| Compd	Spacer	R¹	R²	Metal free Inhibition[a] [%] 1 µM	0.1 µM	IC50[b] [nM]	Zinc complex Inhibition[a] [%] 1 µM	0.1 µM	IC50[b] [nM]	Copper complex Inhibition[a] [%] 1 µM	0.1 µM	IC50[b] [nM]
12	p-xylene			0	n.d.	n.d.	83±2	24±5	n.d.	10±4	n.d.	n.d.
13	m-xylene			0	n.d.	n.d.	31±3	n.d.	n.d.	0	n.d.	n.d.
14	p-xylene			30±4	n.d.	n.d.	87±4	0	n.d.	60±2	n.d.	n.d.
15	m-xylene			33±2	n.d.	n.d.	94±1	13±6	n.d.	80±3	n.d.	n.d.
16	p-xylene			94±4	59±6	n.d.	97±5	28±3	n.d.	98±1	39±3	n.d.
17	m-xylene			95±3	49±9	n.d.	98±4	55±7	n.d.	75±1	n.d.	n.d.
18	p-xylene			32±0.7	n.d.	n.d.	97±6	0	n.d.	52±3	n.d.	n.d.
19	m-xylene			17±5	n.d.	n.d.	91±4	0	n.d.	22±6	n.d.	n.d.
20	p-xylene			89±3	62±3	n.d.	>100	79±1	11	>100	69±3	n.d.
21	m-xylene			89±3	66±3	n.d.	92±3	>100	8.3	>100	88±1	16
22	p-xylene			94±3	86±3	37	99±8	79±0.6	22	85±3	39±3	n.d.
23	m-xylene			58±8	n.d.	n.d.	90±17	37±0.3	n.d.	48±4	n.d.	n.d.
24	p-xylene			3±0.9	n.d.	n.d.	0	n.d.	n.d.	0	n.d.	n.d.
25	m-xylene			4±3	n.d.	n.d.	0	n.d.	n.d.	0	n.d.	n.d.
26	p-xylene			14±2	n.d.	n.d.	10±3	n.d.	n.d.	0	n.d.	n.d.
27	m-xylene			10±3	n.d.	n.d.	10±4	n.d.	n.d.	0	n.d.	n.d.
28	p-xylene			91±0.4	37±0.9	n.d.	97±4	>100	40	57±4	n.d.	n.d.
29	m-xylene			87±2	50±1	n.d.	>100	91±4	52	55±1	n.d.	n.d.
30	p-xylene			0	n.d.	n.d.	14±3	n.d.	n.d.	14±3	n.d.	n.d.
31	m-xylene			24±2	n.d.	n.d.	20±3	n.d.	n.d.	0	n.d.	n.d.
FC-131	cyclo-[D-Tyr-Arg-Arg-Nal-Gly-]			100	100	1.8	–	–	–	–	–	–

[a] CXCR4 binding activity was assessed based on inhibition of [125I]CXCL12 binding to Jurkat cells. Percent inhibition for all compounds at 1 and 0.1 µM were calculated relative to the percent inhibition by FC131 (100%). [b] IC50 values are the concentrations which correspond to 50% inhibition of [125I]CXCL12 binding to Jurkat cells. All data are mean values ±SEM of at least three independent experiments. n.d.=not determined.

affinities is commonly seen for these compounds and their zinc(II) or copper(II) complexes.

We investigated the CXCR4 antagonistic activity of compound 22 and the zinc complexes of 20, 21, 22, and 28, all of which possess strong CXCR4 binding activity. The CXCR4 antagonistic activity was assessed based on the inhibitory activity of the compounds against Ca^{2+} mobilization induced by CXCL12 stimulation through CXCR4 (figure S1 in the Support-

– 274 –
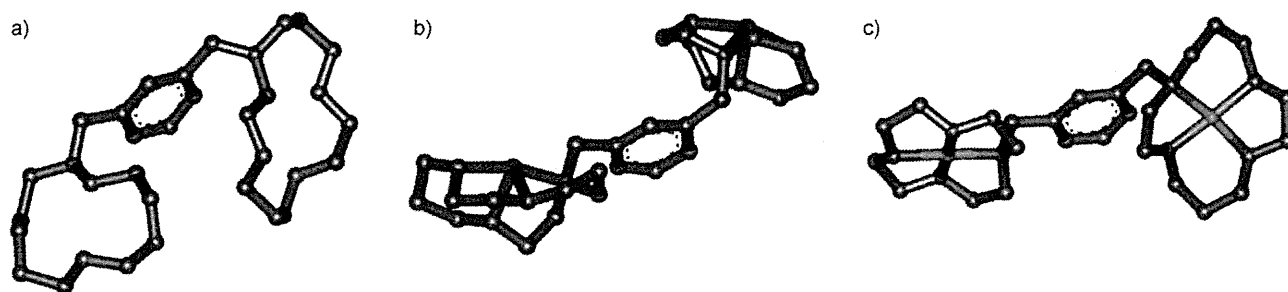
Figure 2. Structures calculated by molecular modeling of a) compound **21**, and its b) zinc and c) copper complexes. Atom color code: nitrogen = blue, carbon = gray, zinc = red, copper = light red.

ing Information). All of the tested compounds showed significant antagonistic activity at 1 μM.

The representative compounds **14, 16, 20–23, 28**, and **29**, as well as their zinc chelates, were evaluated for anti-HIV activity. CXCR4 is the major co-receptor for the entry of T-cell-linetropic (X4) HIV-1.[10,11] Inhibitory activity against X4-HIV-1 (NL4-3 strain)-induced cytopathogenicity in MT-4 cells was assessed and is shown in Table 2.[38] A correlation between CXCR4 bind-

tested compounds exhibited significant cytotoxicity (CC_{50} values > 10 μM; Table 2). Conversely, zinc complexes of **20, 21, 22**, and **28** did not exhibit significant anti-HIV activity against macrophage-tropic (R5) HIV-1 (NL(AD8) strain)-induced cytopathogenicity in PM-1 cells at concentrations below 10 μM. Since R5-HIV-1 strains use CCR5 instead of CXCR4 as the major co-receptor for entry, this suggests that these compounds do not bind CCR5 but rather are highly selective for CXCR4.

Table 2. Anti-HIV activity and cytotoxicity of representative compounds in the metal ion-free and zinc chelates.

Compd	Metal ion-free		Zinc chelate	
	EC_{50}[a] [nM]	CC_{50}[b] [μM]	EC_{50}[a] [nM]	CC_{50}[b] [μM]
14	200	>10	200	>10
16	21	>10	8.2	>10
20	38	>10	39	>10
21	50	>10	36	>10
22	93	>10	48	>10
23	290	>10	220	>10
28	36	>10	56	>10
29	130	>10	42	>10
FC131	93	>10		
AZT	69	>100		

[a] EC_{50} values are the concentrations corresponding to 50% protection from X4-HIV-1 (NL4-3 strain)-induced cytopathogenicity in MT-4 cells. [b] CC_{50} values are the concentrations at which the viability of MT-4 cells is reduced by 50%. All data are mean values from at least three independent experiments.

ing activity and anti-HIV activity was observed. For compound **16** and its zinc complex, anti-HIV activity was significantly stronger than CXCR4 binding activity, and for the zinc complexes of compounds **20–22**, the CXCR4 binding activity is two to four-times stronger than the anti-HIV activity. The anti-HIV activity of the zinc complex of **16** was the most potent ($EC_{50} =$ 8.2 nM). This is comparable to the anti-HIV activities of **16** and its zinc complex that were reported previously.[20,22,42,43] The zinc complex of **21**, which was the most active compound in terms of CXCR4 binding activity, also exhibited potent anti-HIV activity ($EC_{50} = 36$ nM).

Taken together, these results show that all of the compounds exhibiting CXCR4 binding activity also showed significant anti-HIV activity (EC_{50} values < 300 nM), and none of the

Conclusions

The present study introduces a new class of low-molecular-weight CXCR4 antagonists and their zinc(II) or copper(II) complexes, which contain pyridyl or azamacrocycle moieties with p-xylene or m-xylene spacers. These compounds demonstrated strong CXCR4 binding activity. Zinc complexes of **20** and **21**, which were the two most active compounds, contain cyclen and cyclam rings with p- and m-xylene spacers and exhibited remarkably potent IC_{50} values (11 and 8.3 nM, respectively). These compounds showed significant CXCR4 antagonistic activity, based on inhibitory activity against Ca^{2+} mobilization induced by CXCL12 stimulation through CXCR4, as well as potent anti-HIV activity, as assessed by protection from X4-HIV-1-induced cytopathogenicity in MT-4 cells. These results provide useful insights into the future design of novel CXCR4 antagonists, complementing information from other CXCR4 antagonists such as T140, FC131, and KRH-1636. Furthermore, these new compounds are useful for the development of therapeutic strategies for CXCR4-relevant diseases and chemical probes to study the biological activity of CXCR4.

Experimental Section

Chemistry

Compounds **12–17, 20, 21, 24, 25, 27–29**, and **31** were synthesized as previously reported.[20,22,37,40,41,44–47] Compounds **18, 19, 22, 23, 26**, and **30** were synthesized in the present study; details are provided in the Supporting Information. A representative compound, **18**, was synthesized by coupling p-dibromoxylene (1,4-bis-(bromomethyl)benzene) with tri-Boc-protected 1,4,7,10-tetraazacyclododecane, followed by treatment with trifluoroacetic acid and subsequent coupling with bis(pyridin-2-ylmethyl)amine. All crude compounds were purified by RP-HPLC and identified by FAB/ESI-

HRMS. Zinc(II) or copper(II) complex formation was accomplished by treatment of the above compounds with 10 equiv of $ZnCl_2$ or $CuCl_2$ in PBS. All zinc(II) or copper(II) complexes were characterized by chemical shifts of their methylene protons in ^1H NMR analysis. The pyridyl zinc(II) complex was characterized previously,[37] and zinc(II) or copper(II) complex formation with these macrocyclic compounds has been reported elsewhere.[41,42,48,49] Detailed procedures and data are provided in the Supporting Information.

Biological assays

A CXCR4 binding assay for compounds, based on the inhibition of [^{125}I]CXCL12 binding to Jurkat cells, was performed as reported by Tanaka et al.[38] CXCR4 antagonistic activity was evaluated as described by Ichiyama et al[27], measuring inhibitory activity against Ca^{2+} mobilization induced by CXCL12 stimulation in HOS cells expressing CXCR4. Anti-HIV activity was determined by inhibitory activity against X4-HIV-1(NL4–3)-induced cytopathogenicity in MT-4 cells as reported by Tanaka et al.[38] An X4 HIV-1 infectious molecular clone (pNL4–3) was obtained from the AIDS Research and Reference Reagent Program. The virus NL4-3 was obtained from the culture supernatant of 293T cells transfected with pNL4–3.

Molecular modeling

Molecular modeling calculations were performed using Sybyl (version 7.0, Tripos). Energy minimization was performed using the Tripos force field and Gasteiger–Hückel charge parameters. The lowest energy conformation was obtained by random search methods.

Acknowledgements

Keywords: azamacrocycles · Ca^{2+} mobilization · CXCR4 · HIV · structure–activity relationships

[1] T. Nagasawa, H. Kikutani, T. Kishimoto, *Proc. Natl. Acad. Sci. USA* **1994**, *91*, 2305–2309.

[2] C. C. Bleul, M. Farzan, H. Choe, C. Parolin, I. Clark-Lewis, J. Sodroski, T. A. Springer, *Nature* **1996**, *382*, 829–833.

[3] E. Oberlin, A. Amara, F. Bachelerie, C. Bessia, J. L. Virelizier, F. Arenzana-Seisdedos, O. Schwartz, J. M. Heard, I. Clark-Lewis, D. L. Legler, M. Loetscher, M. Baggiolini, B. Moser, *Nature* **1996**, *382*, 833–835.

[4] K. Tashiro, H. Tada, R. Heilker, M. Shirozu, T. Nakano, T. Honjo, *Science* **1993**, *261*, 600–603.

[5] C. C. Bleul, R. C. Fuhlbrigge, J. M. Casanovas, A. Aiuti, T. A. Springer, *J. Exp. Med.* **1996**, *184*, 1101–1109.

[6] K. Tachibana, S. Hirota, H. Iizasa, H. Yoshida, K. Kawabata, Y. Kataoka, Y. Kitamura, K. Matsushima, N. Yoshida, S. Nishikawa, T. Kishimoto, T. Nagasawa, *Nature* **1998**, *393*, 591–594.

[7] T. Nagasawa, S. Hirota, K. Tachibana, N. Takakura, S. Nishikawa, Y. Kitamura, N. Yoshida, H. Kikutani, T. Kishimoto, *Nature* **1996**, *382*, 635–638.

[8] Y. Zhu, Y. Yu, X. C. Zhang, T. Nagasawa, J. Y. Wu, Y. Rao, *Nat. Neurosci.* **2002**, *5*, 719–720.

[9] R. K. Stumm, C. Zhou, T. Ara, F. Lazarini, M. Dubois-Dalcq, T. Nagasawa, V. Hollt, S. Schulz, *J. Neurosci.* **2003**, *23*, 5123–5130.

[10] H. K. Deng, R. Liu, W. Ellmeier, S. Choe, D. Unutmaz, M. Burkhart, P. D. Marzio, S. Marmon, R. E. Sutton, C. M. Hill, C. B. Davis, S. C. Peiper, T. J. Schall, D. R. Littman, N. R. Landau, *Nature* **1996**, *381*, 661–666.

[11] Y. Feng, C. C. Broder, P. E. Kennedy, E. A. Berger, *Science* **1996**, *272*, 872–877.

[12] T. Koshiba, R. Hosotani, Y. Miyamoto, J. Ida, S. Tsuji, S. Nakajima, M. Kawaguchi, H. Kobayashi, R. Doi, T. Hori, N. Fujii, M. Imamura, *Clin. Cancer Res.* **2000**, *6*, 3530–3535.

[13] A. Müller, B. Homey, H. Soto, N. Ge, D. Catron, M. E. Buchanan, T. McClanahan, E. Murphy, W. Yuan, S. N. Wagner, J. L. Barrera, A. Mohar, E. Verastegui, A. Zlotnik, *Nature* **2001**, *410*, 50–56.

[14] H. Tamamura, A. Hori, N. Kanzaki, K. Hiramatsu, M. Mizumoto, H. Nakashima, N. Yamamoto, A. Otaka, N. Fujii, *FEBS Lett.* **2003**, *550*, 79–83.

[15] N. Tsukada, J. A. Burger, N. J. Zvaifler, T. J. Kipps, *Blood* **2002**, *99*, 1030–1037.

[16] J. Juarez, K. F. Bradstock, D. J. Gottlieb, L. J. Bendall, *Leukemia* **2003**, *17*, 1294–1300.

[17] T. Nanki, K. Hayashida, H. S. El-Gabalawy, S. Suson, K. Shi, H. J. Girschick, S. Yavuz, P. E. Lipsky, *J. Immunol.* **2000**, *165*, 6590–6598.

[18] H. Tamamura, M. Fujisawa, K. Hiramatsu, M. Mizumoto, H. Nakashima, N. Yamamoto, A. Otaka, N. Fujii, *FEBS Lett.* **2004**, *569*, 99–104.

[19] T. Murakami, T. Nakajima, Y. Koyanagi, K. Tachibana, N. Fujii, H. Tamamura, N. Toshida, M. Waki, A. Matsumoto, O. Yoshie, T. Kishimoto, N. Yamamoto, T. Nagasawa, *J. Exp. Med.* **1997**, *186*, 1389–1393.

[20] D. Schols, S. Struyf, J. Van Damme, J. A. Este, G. Henson, E. DeClarcq, *J. Exp. Med.* **1997**, *186*, 1383–1388.

[21] B. J. Doranz, K. Grovit-Ferbas, M. P. Sharron, S.-H. Mao, M. Bidwell Goetz, E. S. Daar, R. W. Doms, W. A. O'Brien, *J. Exp. Med.* **1997**, *186*, 1395–1400.

[22] G. A. Donzella, D. Schols, S. W. Lin, J. A. Este, K. A. Nagashima, *Nat. Med.* **1998**, *4*, 72–76.

[23] O. M. Z. Howard, J. J. Oppenheim, M. G. Hollingshead, J. M. Covey, J. Bigelow, J. J. McCormack, R. W. Buckheit, Jr., D. J. Clanton, J. A. Turpin, W. G. Rice, *J. Med. Chem.* **1998**, *41*, 2184–2193.

[24] H. Tamamura, Y. Xu, T. Hattori, X. Zhang, R. Arakaki, K. Kanbara, A. Omagari, A. Otaka, T. Ibuka, N. Yamamoto, H. Nakashima, N. Fujii, *Biochem. Biophys. Res. Commun.* **1998**, *253*, 877–882.

[25] H. Tamamura, A. Omagari, S. Oishi, T. Kanamoto, N. Yamamoto, S. C. Peiper, H. Nakashima, A. Otaka, N. Fujii, *Bioorg. Med. Chem. Lett.* **2000**, *10*, 2633–2637.

[26] N. Fujii, S. Oishi, K. Hiramatsu, T. Araki, S. Ueda, H. Tamamura, A. Otaka, S. Kusano, S. Terakubo, H. Nakashima, J. A. Broach, J. O. Trent, Z. Wang, S. C. Peiper, *Angew. Chem.* **2003**, *115*, 3373–3375; *Angew. Chem. Int. Ed.* **2003**, *42*, 3251–3253.

[27] K. Ichiyama, S. Yokoyama-Kumakura, Y. Tanaka, R. Tanaka, K. Hirose, K. Bannai, T. Edamatsu, M. Yanaka, Y. Niitani, N. Miyano-Kurosaki, H. Takaku, Y. Koyanagi, N. Yamamoto, *Proc. Natl. Acad. Sci. USA* **2003**, *100*, 4185–4190.

[28] H. Tamamura, N. Fujii, *Curr. Drug Targets-Infectious Disorders* **2004**, *4*, 103–110.

[29] H. Tamamura, K. Hiramatsu, S. Ueda, Z. Wang, S. Kusano, S. Terakubo, J. O. Trent, S. C. Peiper, N. Yamamoto, H. Nakashima, A. Otaka, N. Fujii, *J. Med. Chem.* **2005**, *48*, 380–391.

[30] H. Tamamura, T. Araki, S. Ueda, Z. Wang, S. Oishi, A. Esaka, J. O. Trent, H. Nakashima, N. Yamamoto, S. C. Peiper, A. Otaka, N. Fujii, *J. Med. Chem.* **2005**, *48*, 3280–3289.

[31] G. C. Valks, G. McRobbie, E. A. Lewis, T. J. Hubin, T. M. Hunter, P. J. Sadler, C. Pannecouque, E. De Clercq, S. J. Archibald, *J. Med. Chem.* **2006**, *49*, 6162–6165.

[32] W. Zhan, Z. Liang, A. Zhu, S. Kurtkaya, H. Shim, J. P. Snyder, D. C. Liotta, *J. Med. Chem.* **2007**, *50*, 5655–5664.

[33] A. Khan, G. Nicholson, J. Greenman, L. Madden, G. McRobbie, C. Pannecouque, E. De Clercq, R. Ullom, D. L. Maples, R. D. Maples, J. D. Silversides, T. J. Hubin, S. J. Archibald, *J. Am. Chem. Soc.* **2009**, *131*, 3416–3417.

[34] G. J. Bridger, R. T. Skerlj, P. E. Hernandez-Abad, D. E. Bogucki, Z. Wang, Y. Zhou, S. Nan, E. M. Boehringer, T. Wilson, J. Crawford, M. Metz, S. Hatse, K. Princen, E. De Clercq, D. Schols, *J. Med. Chem.* **2010**, *53*, 1250–1260.

[35] R. T. Skerlj, G. J. Bridger, A. Kaller, E. J. McEachern, J. B. Crawford, Y. Zhou, B. Atsma, J. Langille, S. Nan, D. Veale, T. Wilson, C. Harwig, S. Hatse, K. Princen, E. De Clercq, D. Schols, *J. Med. Chem.* **2010**, *53*, 3376–3388.

[36] M. Takenaga, H. Tamamura, K. Hiramatsu, N. Nakamura, Y. Yamaguchi, A. Kitagawa, S. Kawai, H. Nakashima, N. Fujii, R. Igarashi, *Biochem. Biophys. Res. Commun.* **2004**, *320*, 226–232.

[37] H. Tamamura, A. Ojida, T. Ogawa, H. Tsutsumi, H. Masuno, H. Nakashima, N. Yamamoto, I. Hamachi, N. Fujii, *J. Med. Chem.* **2006**, *49*, 3412–3415.

[38] T. Tanaka, H. Tsutsumi, W. Nomura, Y. Tanabe, N. Ohashi, A. Esaka, C. Ochiai, J. Sato, K. Itotani, T. Murakami, K. Ohba, N. Yamamoto, N. Fujii, H. Tamamura, *Org. Biomol. Chem.* **2008**, *6*, 4374–4377.

[39] G. J. Bridger, R. T. Skerlj, D. Thornton, S. Padmanabhan, S. A. Martellucci, G. W. Henson, M. J. Abrams, N. Yamamoto, K. De Vreese, R. Pauwels, E. De Clercq, *J. Med. Chem.* **1995**, *38*, 366–378.

[40] G. J. Bridger, R. T. Skerlj, S. Padmanabhan, S. A. Martellucci, G. W. Henson, M. J. Abrams, H. C. Joao, M. Witvrouw, K. De Vreese, R. Pauwels, E. De Clercq, *J. Med. Chem.* **1996**, *39*, 109–119.

[41] Y. Inouye, T. Kanamori, T. Yoshida, T. Koike, M. Shionoya, H. Fujioka, E. Kimura, *Biol. Pharm. Bull.* **1996**, *19*, 456–458.

[42] L. O. Gerlach, J. S. Jakobsen, K. P. Jensen, M. R. Rosenkilde, R. T. Skerlj, U. Ryde, G. J. Bridger, T. W. Schwartz, *Biochemistry* **2003**, *42*, 710–717.

[43] H. F. Egberink, E. De Clercq, A. L. Van Vliet, J. Balzarini, G. J. Bridger, G. Henson, M. C. Horzinek, D. Schols, *J. Virol.* **1999**, *73*, 6346–6352.

[44] M. Le Baccon, F. Chuburu, L. Toupet, H. Handel, M. Soibinet, I. Dechamps-Olivier, J.-P. Barbier, M. Aplincourt, *New J. Chem.* **2001**, *25*, 1168–1174.

[45] B. Antonioli, D. J. Bray, J. K. Clegg, K. Gloe, K. Gloe, O. Kataeva, L. F. Lindoy, J. C. McMurtrie, P. J. Steel, C. J. Sumby, M. Wenzel, *Dalton Trans.* **2006**, 4783–4794.

[46] S. P. Foxon, D. Utz, J. Astner, S. Schindler, F. Thaler, F. W. Heinemann, G. Liehr, J. Mukherjee, V. Balamurugan, D. Ghosh, R. Mukherjee, *Dalton Trans.* **2004**, 2321–2328.

[47] S. Mandal, F. Lloret, R. Mukherjee, *Inorg. Chim. Acta* **2009**, *362*, 27–37.

[48] M. Soibinet, I. De'champs-Olivier, E. Guillon, J.-P. Barbier, M. Aplincourt, F. Chuburu, M. Le Baccon, H. Handel, *Eur. J. Inorg. Chem.* **2003**, 1984–1994.

[49] R. W. Hay, M. T. Tarafder, *Transition Met. Chem.* **1990**, *15*, 490–492.

Fluorescence-Quenching Screening of Protein Kinase C Ligands with an Environmentally Sensitive Fluorophore

Wataru Nomura,[†] Nami Ohashi,[†] Yoshiaki Okuda,[†,‡] Tetsuo Narumi,[†] Teikichi Ikura,[‡] Nobutoshi Ito,[‡] and Hirokazu Tamamura*,[†,‡]

[†]Department of Medicinal Chemistry, Institute of Biomaterials and Bioengineering, Tokyo Medical and Dental University, 2-3-10 Kandasurugadai, Chiyoda-ku, Tokyo 101-0062, Japan

[‡]Graduate School of Biomedical Science, Tokyo Medical and Dental University, 1-5-45 Yushima, Bunkyo-ku, Tokyo 113-8510, Japan

S Supporting Information

ABSTRACT: A novel fluorescence-quenching screening method for protein kinase C (PKC) ligands was developed utilizing solvatochromic fluorophores. Solvatochromic dyes, highly sensitive to the presence or the absence of competitive ligands in their binding to the C1b domain of PKCδ (δC1b), were combined with a known pharmacophoric moiety of 1,2-diacylglycerol (DAG) lactones, PKC ligands. Addition of δC1b to the fluorescent compounds caused a gradual increase in the fluorescent intensity in proportion to the increase of δC1b. As a competitive ligand was added to the complex of δC1b domain and fluorescent compounds, a gradual decrease in the fluorescent intensity was observed. The relative binding affinities of known ligands were successfully determined by this fluorescent method and corresponded well to the K_i values measured by a radioisotope method. These results indicate that washing, which is a laborious step in binding evaluations, is not required for this environmentally sensitive fluorophore based system. Screening with the system was performed for 2560 preselected library compounds with possible pharmacophores, and some lead compounds were found. This fluorescence-based method could be applied widely to known ligand—receptor combinations.
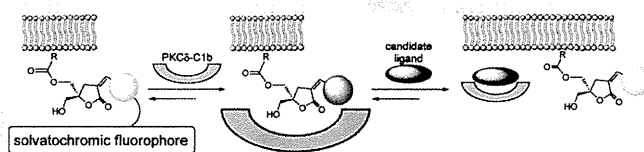
■ INTRODUCTION

Solvatochromic fluorophores are sensitive to immediate changes in their environment such as binding of ligands to proteins,[1] and significant biological issues have been examined by chemical probes with fluorescent dyes.[2,3] The major advantage of the fluorescence-based methods in the observation of physiological phenomena in cells is that detection and evaluation can be performed in real-time directly by microscopy. In these techniques, the signal/background ratio is critical to avoid the observation of artifacts or to obtain clearer images at high resolution. Screening methods of bioactive compounds have been developed as another application of fluorescence.[4] From the aspect of sensitivity, radioisotope (RI) based methods are more efficient but involve laborious experimental procedures. For the development of convenient screening procedures, a simple method for evaluation of binding is needed. By attachment of solvatochromic fluorophores to known ligands, the binding affinity of unknown ligands can be evaluated and related to RI methods.[5] Fluorescent intensity is highly dependent on the binding state to a target protein, and the signal/background ratio would be sufficient without washing steps, which are normally necessary in fluorescent analysis.[6,7]

In this study, we have developed reporter compounds containing solvatochromic dyes for the detection of ligand binding to a target protein and applied them to the screening of chemical libraries. Protein kinase Cδ (PKCδ) was chosen as a target

protein because of its importance in physiological phenomena. The 11 isozymes that constitute PKC play pivotal roles in physiological responses to growth factors, oxidative stress, 1,2-diacylglycerol (DAG), and tumor promoters, such as phorbol esters. These responses regulate numerous cellular processes,[8,9] including proliferation,[10] differentiation,[11] migration,[12] and apoptosis.[13,14] Membrane translocation of PKC is caused by binding of ligands to the C1b domain and has been recognized as an important phenomenon in signal transduction because the localization of PKC is key in determining isozyme-specific functions by defining binding partners for downstream signaling.[15] Despite the complex regulatory mechanisms of PKC activation, considerable progress has been made in understanding isozyme-specific functions[16] and several ligands with high specificity for PKC isozymes have been developed as potential drugs.[17−23] Through the development of DAG-lactones, whose design is based on the endogenous ligand DAG, the importance of maintaining intact the pharmacophore triad of two carbonyl groups (sn-1 and sn-2) and the primary alcohol has been established as a requirement in high affinity ligands for PKC (Figure 1).[16] Various PKC ligands have been synthesized and found to be inhibitors of tumor promotion or of other diseases.